E-ISSN : 2541-5794
P-ISSN : 2503-216X

Journal of Geoscience, Engineering, Environment, and Technology
Vol 9 No 4 2024

RESEARCH ARTICLE

Volcanic Evolution of the Southern Mountain Neogene Magmatic Belt in Baturagung Range Central Java, Indonesia

Sri Mulyaningsih[1,*], Rahel Putong[1], Anka Prima[1], Radhtya Adzan Hidayah[1], Desi Kiswiranti[1]
[1]*Geological Engineering Department, Akprind University, Jl. Kalisahak No. 28 Balapan Yogyakarta, Indonesia, 55222.*

* Corresponding author : sri_m@akprind.ac.id
Tel.:+62-821-3629-3027; fax: +62-274-563847
Received: Jul 29, 2024. Accepted: Nov 21, 2024
DOI: 10.25299/jgeet.2024.9.04.18461

Abstract

Various Neogene volcanic rocks associated with calcareous sediments compose the Southern Mountain located from Imogiri at Yogyakarta to Wonogiri at Central Java, Indonesia. The volcanic rocks are concentrated along the north side of the Mountains which was recognized as the Neogene magmatic arc of Java; Baturagung is part of them. The discussion focuses on the relationship between the volcanic features and its basin evolution. The methods were geological fieldwork including measuring sections and collecting samples, thin sections, XRF, AAS, and micropaleontology. More than 13 circular hogbacks, circular valleys, and domes are observed based on the SRTM image. The petrology observed pyroxene-rich basaltic volcanic rocks, dacitic volcanic rocks, andesitic volcanic rocks, coral-rich volcanic breccia. From the bottom to the top, its stratigraphy of the Kebo-Butak Formation that notes basaltic volcanic rocks, pumice-rich lapillistone, and tuff of Early Neogene (before P4-N6) with muddy sandstone above the basalts of N 5-6 (Lower Miocene). The Semilir Formation consists of pumice-rich and dacitic tuff. Andesitic volcanic rocks of the Nglanggeran Formation with inlayer of marl of N 13-14. In the volcanic rocks trace elements show REE-rich (84-140 ppm), higher mobile elements of Sr (~480-602 ppm), medium Rb (22.2-23.7 ppm), and medium La (12-21 ppm), and wide range of immmobile trace elements of Nb ~2.7-7.9 ppm, Zr ~53-171 ppm, P ~840-1300 ppm, higher Ti (4400-4900 ppm), and higher Vanadium (V) of 92-302 ppm. Plot TiO_2 vs. Al_2O_3 into the volcanic rocks indicates those were volcanism within plate boundaries. Plot Ta/Th vs Th/Hf shows continental extensional volcanism to continental arc margin. Plot Nb/Zr vs. Th/Zr explains the transitional zone to continental arc volcanism. The spider diagram shows Rb, Ce, P, Ti, Sr, Zr, and Y strongly metasomatized as a result of the upper continental arc. The chondrite normalized REE shows negative trends for Tb, Tm, Lu, Sm, and Eu and positive trends for Ce, Gd, Zr, and Y, which indicate superimposed volcanism under a submarine environment during the Neogene Period. Stratigraphic sections inform were periodically active volcanism. The Kebo-Butak Formation was formed by multiple volcanoes, some of which were active simultaneously while others were not, though both fall within the Early Neogene age range. Similarly, the Semilir and Nglanggeran Formations were also formed by volcanic activity from several volcanoes that were active at different times and overlapped with each other.

Keywords: formation, volcanism, evolution, basin, Neogene

1. Introduction

Ellipsoidal domes and circular valleys with hogback geomorphologies varying dimensions in the ranges of a couple of hectares until vews acres are identified using an SRTM image of the Southern Mountain (Central Java-Indonesia) (Fig. 1). Three prominent types of volcanic rocks associated with calcareous sediments were observed by the previous publications, composed of pyroxene-rich andesitic volcanic rocks, pumice-rich dacitic volcanic rocks, and andesitic volcanic rocks with marls, calcareous sandstones, and limestones (Baba et al., 2022; Bronto et al., 2009; Mulyaningsih, 2013; Setijadji et al., 2006). The older publications reccorded Baturagung Range stratigraphy, from the bottom to the top, are the basement of Cretaceous metamorphic rocks (schist, phylite, and marble) of Jiwo Formation; beds of limestone and sandstone of the Eocene Gamping-Wungkal Formation; the Late Oligocene to Early Miocene volcanic rocks of the Kebo-Butak, Semilir, and Nglanggeran Formations; and the Middle Miocene submarine sedimentary rocks of the Sambipitu, Oyo, and Wonosari Formations (Rahardjo et al., 1995b), (Surono et al., 1992), (Adli et al., 2018; Agastya; et al., 2018; Bachtiar et al., n.d.; Barianto et al., 2010; Mulyaningsih et al., 2011). It can be interpreted that this area was developed by volcanism and marine activities during the Neogene period.

Discuss about the volcanism, some researchers decided Southern Mountain originated from volcanic to subvolcanic turbiditic processes (Clements et al., 2009; Clements and Hall, 2007; Romario et al., 2015). Conversely, others propose Java evolved as an island arc, formed through multiple episodes of Cenozoic arc magmatism (Setijadji et al., 2006)(Smyth et al., 2008). Classical turbidite originated by forearc basin develop-ments related to these volcanic rocks were discussed by (Ardine et al., 2022; Chen et al., 2017; Patria et al., n.d.; RAHMAD et al., 2017; Surono, 2008). So that it's concluded that debating in their deposition and geological developments are still occured.

Discussing about the submarine volcanism, basaltic lava with pillow structures were described in many places, including Berbah (Bronto et al., n.d.; Faizal et al., 2018; Mulyaningsih et al., 2006), Gedangsari (Nugrahini et al., 2019, 2017), Bayat and Giriloyo (Imogiri) (Bronto, 2010; Mulyaningsih, 2016). Pillow lava is interpreted as a deep marine volcanic rock with a high-pressure and low-temperature environment. Beds of black tuff, greenish-yellow tuff, and foram-rich calcareous sediments of the Kebo-Butak Formation have been extensively discussed in previous publications, indicating it was deposited during the Late Oligocene (26.93 Ma) to Early Miocene (23.06 Ma) (Akmaluddin et al., 2024; Goncalves and Mulyaningsih, 2015; Mulyaningsih et al., 2019; Novita et al., 2014). The

Kebo-Butak dacitic volcanic rocks and the Semilir ryolitic volcanic rocks have been extensively reported in the previous publications, suggesting a destructive volcanic origin (Patria et al., n.d.), (Mulyaningsih, 2016) and some others by gravity flows of turbiditic epiclastic deep marine sequential (Ardine et al., 2022; Chen et al., 2017; RAHMAD et al., 2017), (Kusumayudha et al., 2023; Novianto et al., 2020; RODHI et al., 2016). The data described those fragmented volcanic rocks are widely distributed within hundreds kilometers square and hundreds meters of thickness; it's from Parangtritis-Imogiri (west) until Pacitan-Ponorogo (east) so that there were very explosive eruptions in many places or by a very violent volcanic eruption at that time.

The youngest volcanic rocks is andesitic agglomerate, lava, breccia, dikes, and tuff of the Lower Miocene Nglanggeran Formation (Surono et al., 1992). Some publications concluded these rocks were deposited by many volcanos superimposed with the older volcanic formations (Mulyaningsih et al., 2019), (Soviana et al., 2020a), and (Mulyaningsih, 2019). (Sheth et al., 2002) argue that not all orogenic andesites are calc-alkaline series, and conversely, not all calc-alkaline andesites are orogenic. Therefore, prudence is essential when interpreting ancient terrains with complex geology and calc-alkaline rocks as former subduction zones. As argued by most researchers in the Southern Mountains (Smyth et al., 2008), (Cottam et al., 2010), (Clements and Hall, 2007), (Clements et al., 2009), (Nugraha and Hall, 2012) that it was a volcanic arc-related subduction zone. This study discusses volcanism relating to the different types of basaltic andesite, dacitic, and anesitic volcanic rocks that are exposed in the study area. By those deposits, hypothesized calc-alkaline products in a longer period, which was resulting superimposed volcanism.

In a similar subduction tectonic setting, the basaltic-andesitic volcanic rocks and others are likely to belong to the Calc-alkaline magma series, which will be further evidenced by the enrichment of Light Rare Earth Elements (LREEs) and depletion of Heavy Rare Earth Elements (HREEs). Studies of the present volcanos such as Merapi, Agung, and Krakatau reported enrichment of LREE and a slight depletion in HREE in subduction-related volcanic rocks, higher potassium content, and highlighting amphibole fractionation as a significant process in their geological development Volcanos (Del Marmol, 1990), (Nandaka et al., 2023), (Harjono et al., 1989), (Wulaningsih et al., 2013).

Pumice-rich dacitic to rhyolitic volcanic rocks are known as highly fragmented materials that developed by very explosive eruptions (Mulyaningsih, 2015). Historical explosive eruptions in an Indonesian volcanic arc occurred the eruption of Krakatau in 1883 (Dörries, 2003) (Spicak et al., 2008) and the Tambora in 1815 (Self et al., 1984). (Dahren et al., 2012) determined magma plumbing occurred by the 1883 Kratatau's eruption. They recorded clinopyroxene that should be crystallized at depths of 7-12 km and plagioclase that can be formed at shallow crustal (3-7 km), while it known that sub-Moho having a depth of 23-28 km. Those suggest that in caldera-forming eruption, magma can plumbing from the shallow crust.

As a present volcano that relates to a subduction zone, the calc-alkaline magmas of Agung Volcano resulted from partial melting due to the subduction, producing basalt to dacite, enrichments occurred in Rb, Ba, Th, K, and La-Sm, and depletion occurred in Eu-Lu by convergent plate boundaries that are influenced by continental arcs (Syafitri et al., 2022). A calk-alkaline of the Dalli Subvolcano (Urumieh-Dokhtar Magmatic Arc) exhibits enrichments in light REEs and relatively flat to gently upward-sloping profiles for the middle to heavy REEs as attributed to the amphibole fractionation and plagioclase crystallization (Ayati et al., 2013). The Sabzevar Eocene calc-alkaline volcanism (Central Iran) observed hornblende-controlled fractionation and replenishment-fractional crystallization (Lucci et al., 2016), so that occurred in the Arabian-Nubian Shield (Abuamarah et al., 2021), Kaboudarahang-Hamedan (Khalaji, 2020), and Kastamonu (Peccerillo and Taylor, 1976). As discussed above, employing a stratigraphic approach, the study examines the volcanic characteristics and basin evolution of the Southern Mountains. It hypothesizes submarine volcanism involving both constructive and destructive volcanic activities during the Cenozoic.

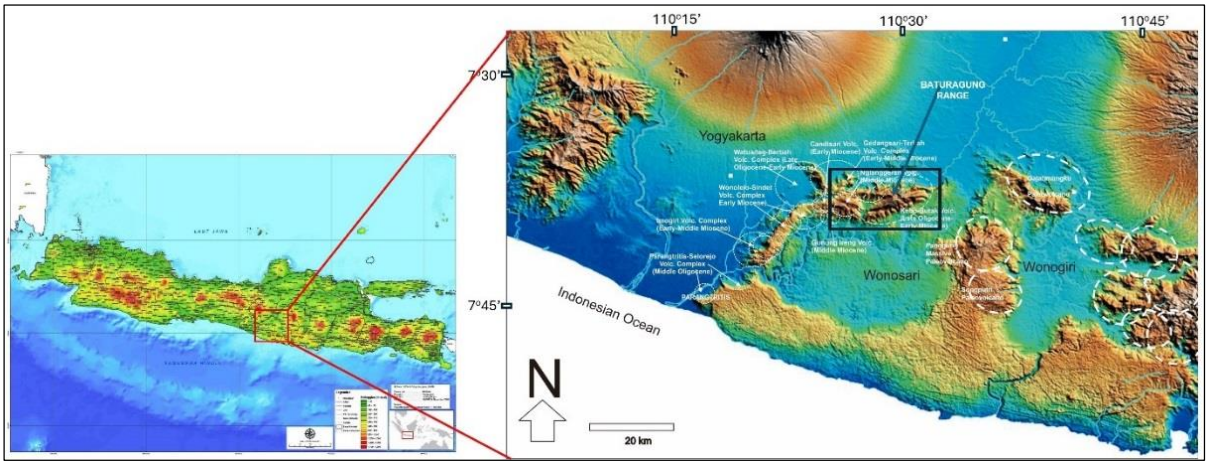

Fig 1. Ellipsoidal domes and circular hogbacks shown under the SRTM image occurring in the Southern Mountain, Central Java-Indonesia, especially in the Baturagung Range (box)

2. Geological Setting

The study area is located within the Southern Mountains, which previous publications described as shaped by the uplift of the Neogene (Tertiary) volcanic belt (van Bemmelen, 1949) (Smyth et al., 2007). Previous studies published different stratigraphy, that is divided into three zones (Table 1): the Imogiri-Parangtritis Zone (western) according to (Rahardjo et al., 1995a), the Patuk-Wonosari Zone including Bayat, and Baturagung Range (middle) according to (Surono et al., 1992), and the Wonogiri-Pacitan-Ponorogo (eastern) according to (Samodra et al., 1992) and (Surono et al., 1992). The study area is in the Baturagung Range (middle zone).

Table 1. Regional stratigraphic of the Southern Mountain, compiled from previous studies (Rahardjo et al., 1995b), (Surono et al., 1992), and (Samodra et al., 1992).

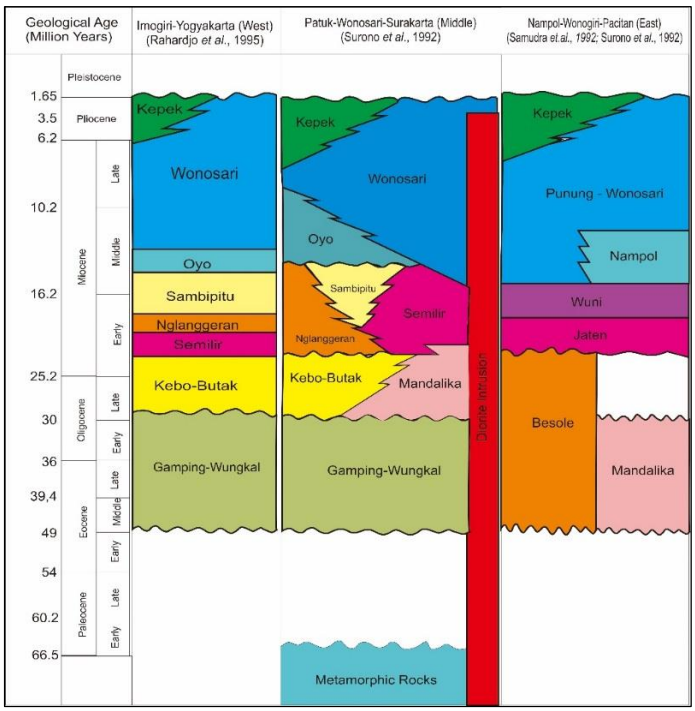

There are the Cretaceous metamorphic rocks and the Gamping-Wungkal Formation that exposed in Jiwo Hills (Bayat District, Klaten Regency, Central Java) (Akmaluddin et al., 2024), (Mulyaningsih, 2016), (Bronto, 2010), and (Novita et al., 2014), north of the study area. Those rocks are intruded by pyroxene-rich diorite, basalt dikes, and andesite sills that were interpreted as volcanic origin (Bronto, 2010) of the active continental margin volcanism (Sutarto and Soesilo, 2020). As reported by (Akmaluddin et al., 2024) and (Novita et al., 2014), known that submarine deposits of the lower Gamping-Wungkal Formation, which is composed of the Eocene marl and sandstone, *Numulites*-rich limestone covering the Cret. metamorphic rocks. Those deposits are also associated with phyllite, shale, and meta-limestone exposed at Jokotuo (Jiwo Hills). Those sedimentary formations might be the basement rocks of the study area.

Very deformed thick layers of zeolite and basalt lava with pillow structures of the Late Oligocene Kebo-Butak Formation were reported by (Rohayati et al., 2017), (Melaningtyas et al., 2019) at Bayat, (Adli et al., 2018) at Ponorogo, and (Baba et al., 2022) at Pacitan indicate that the dynamic basin developments occurred related to the volcanism phase since the Oligocene. Those linear with the arguments of (Mulyaningsih, 2016) and (Smyth et al., 2008) that in the Early Southern Mountain developments were deep marine volcanism in the wide areas.

Two types of pumice-rich volcanic rocks are known in the Southern Mountain of the Upper Kebo-Butak and the Semilir Formations with a very light grey, greenish grey, to yellowish-grey, and varying in thickness from a few meters to in hundred meters (Chen et al., 2017), (Bronto et al., 2009), (Mulyaningsih et al., 2019), (Patria et al., n.d.), (RAHMAD et al., 2017), (Ardine et al., 2022), and (Surono, 2008). (Husadani et al., n.d.) reported layers of planktonic-rich mudstone (below the pumice-rich tuff) at Pucung (Imogiri) having an age of N5-9 (Early Miocene), (Mulyaningsih et al., 2019) described thin layers of calcareous claystone exposed between the black tuff layers and the beds of andesitic tuff at Cengkehan-Giriloyo (Imogiri) having an age of P4-N6 (Late Oligocene-Early Miocene), (Irawan et al., 2009) also described layers of muddy sandstone deposited between the greenish pumice-rich basaltic tuff and the pyroxene-rich andesitic breccia with lava, which is exposed at Sindet (Jetis District, Bantul Regency) having an age of N 6-8 (Early Miocene). Dacitic dikes are exposed at Plencing (Gunung Gedhe) as part of the Semilir Formation cutting the greenish pumice-rich volcanic rocks (Irawan et al., 2009). The dynamic of magmatic arc volcanism depositing fragmented volcanic rocks, coherent lava, and dikes were occured in the Late Oligocene till Upper Early Miocene.

Andesitic agglomerate and breccia of the Nglanggeran Formation exposed at Gunung Nglanggeran were reported by (Salim, 2020), (Razi, 2018), and (Soviana et al., 2020b). Those deposits are also found at Wediombo (Hartono and Bronto, 2007) and (Paryani and Haryono, 2022). These volcanic rocks are associated with less fragmented volcanic materials, i.a dike, sill, lava, autoclatic breccia, and tuff. (Soeria-Atmadja et al., 1994) reported those volcanic rocks varied in age from Paleocene (40 Ma) till Late Miocene (~9 Ma), varying in composition from basaltic to andesitic, and very wide distribution from Parangtritis in the west to Trenggalek in the east. During the Late Paleocene to Late Miocene, the dynamic volcanism of effusive and explosive volcanic eruptions intersected within so many volcanoes in the Southern Mountains.

Epiclastic volcanic origin of the Sambipitu Formation and the Oyo Formation were gradually developed in line with the decreasing volcanism. and the Wonosari Formation, all of which were deposited within submarines starting from bathyal, neritic, and transition.

The last formation in the Southern Mountain is the Wonosari Formation, characterized by the presence of thick beds of clastic and non-clastic limestone, as documented by (Romario et al., 2015) and (Nugrahini et al., 2017), (Nugraha and Hall, 2012), see Fig. 2. The volcanic rocks exposed on Gunung Ireng are attributed to the Nglanggeran Formation, while the calcareous sediments are identified as part of the Oyo Formations. This distinction underlines the Southern

Mountain's classification as a Submarine Neogene Volcanic Arc, a geological era that spanned from the Late Oligocene to the Middle Miocene, in line with research by (Cottam et al., 2010) and (Clements et al., 2009). The distribution of geological structures in the region is predominantly influenced by oblique normal faults trending southwest-northeast, with their development closely tied to volcanic activity and subsequent uplift (as illustrated in Fig. 2). This observation underscores the dynamic and evolving nature of geological processes that have shaped the Southern Mountain over an extended period.

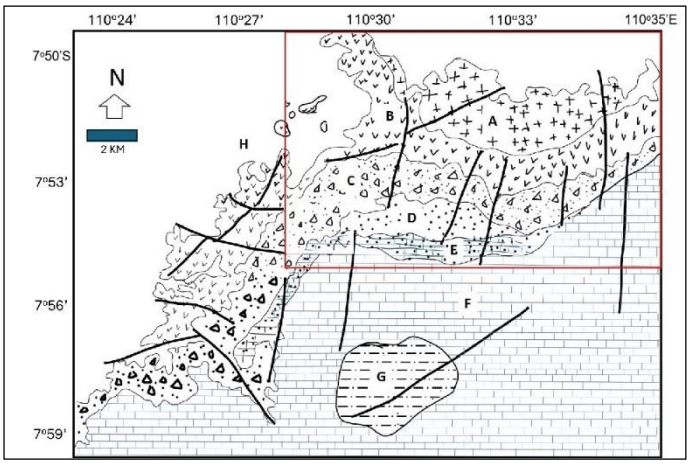

Figure 2. Regional geology of the Baturagung Range (red box) compiled from the previous study; A: Kebo-Butak Form, B: Semilir Form; C: Nglanggeran Form; D: Sambipitu Form; E: Oyo Form; F: Wonosari Form; G: the Kepek Member (of the Wonosari Form.); and H: Alluvial Deposits (Rahardjo, Sukandarrumidi & Rosidi, 1995); (Husadani, et al., 2009); and (Mulyaningsih, et al., 2009)

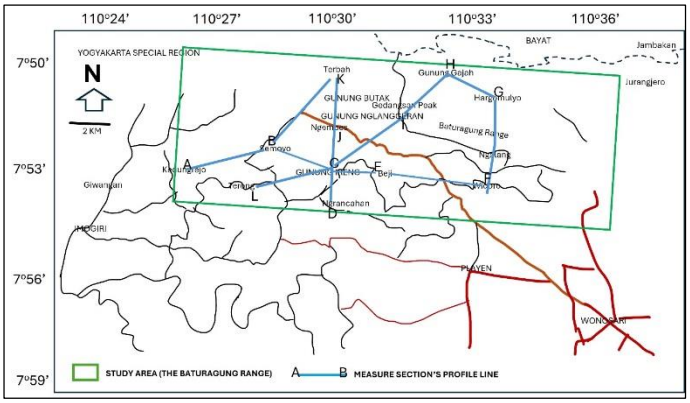

Fig. 3. The measuring sections map

3. Methods and Materials

To analyze the geomorphology, it employed a combination of Digital Elevation Model (DEM) and on-site field observations. It established measurement sections and traversed the geological dome in all cardinal directions, encompassing its outermost boundaries, deepest valleys, and central cores. Specifically, we undertook the following transects: a north-south section of Semoyo (Pathuk, Gunungkidul Regency)–Kedungrejo (Wonolelo, Bantul Regency), an east-west section from Widoro (Gedangsari)–Beji (Patuk, Gunung Kidul Regency), and a southeast-northwest section of Ngembes (Patuk) – Terong (Bantul Regency) (Fig. 3).

The micropaleontological component of the study involved meticulous examination under a stereo microscope at 100x magnification that applied for the calcareous sediments. These samples were collected from each cardinal direction, totaling nine (9) samples. The sampling encompassed the lower layer of calcareous sandstone above the basaltic volcanic rocks, the intermediate marl above the calcareous sandstone, and the upper units of marl and calcarenite. The preparation was started with crushed them using a soft hammer and washed them using a hydrogen peroxide (H_2O_2). Contents of planktic fossils were applied for age interpretation following the Blow Zonation and the benthic foram helped in determining the environmental deposition according to the Postuma Zonation. As much as twelve samples were for thin-section analysis, eight samples were assessed for the major elements, trace elements, and rare earth elements. Thin sections were carefully prepared, polished to dimensions of 2.5x3x5 cm, and reduced to a thickness of 0.003 mm. Subsequently, we examined these thin sections under a polarizing microscope at a magnification of 200x. Trace and rare earth elements were analyzed using an Inductively Coupled Plasma Mass Spectrometry (ICP-MS) and major elements were assessed using X-ray Fluorescence (XRF).

Finally, we diligently observed, measured, and documented the geological structures in the area, which encompassed faults, joints, and dikes. To enhance our analysis, we used the Dip® application for polarization and further interpretation of these structures.

4. Results

4.1. Stratigraphy and Geomorphology

The sections were collected from the north to the south across the Baturagung Range and described as basaltic lava, dike, and sill (Fig. 4.a), distinguished by dark to reddish grey,

vesicular, and porphyritic. Those are composed of augite, labradorite, and glass. Some of them are often together with breccia and tuff, well exposed on the northern flank of Baturagung, i.e. Hargomulyo, Terbah, Gunung Gajah, and Gunung Butak. Overlaying the igneous rocks are layers of green shale and tuff that are mostly folded and deformed (Fig. 4). Beds of black tuff and basaltic lava overlie the igneous rocks (exposed at Gunung Gajah). Some outcrops appear brown and greenish-yellowish grey presenting chlorite and illite (Sumberan: JG, Fig. 3, Gedangsari: IG, Fig 3), but other outcrops consist of crystal-rich tuff exposed at Tegalrejo-Terbah (Gedangsari). The same volcanic rocks are also found at Muntuk and Mangunan (Dlingo, Bantul Regency) and the lower flank of Sudimoro Mount (Imogiri, Bantul Regency) (. Above are thick beds of brown tuff such as exposed at Cengkehan-Cinomati and thin layerings to laminations of white tuff such as exposed at Tegalrejo and Hargomulyo. A layer of the lower formation exposed at Jumbleng River (near Tegalrejo) noted *Ga. ciperoensis*, *Catapsydrax dissimilis*, and *Gs. primordius*, the same description by Rahardjo (2007) at Gunung Pegat, Watugajah, and Pututmati giving an age of P22-N4 (Late Oligocene-Early Miocene) in (Mulyaningsih et al., 2019). It's relevant to (Smyth et al., 2008) that have dated the pumice-rich lapillistone of the Kebo-Butak Formation, and then got the results of 33.5-21 Ma. At the southwestern slope of the Baturagung Range, a layer of basal conglomerate exposed at Candisari (Prambanan), basal breccia with basalt, pumice, and coral fragments exposed at Terbah, calcareous sandstone and mudstone containing foram fragments showing N5-6 (Lower Miocene) exposed at western slope of Gunung Butak, Cengkehan, and Pucung-Wonolelo, and breccia with basalt fragments and tuff matrix exposed at Sumber (Berbah). Those sediments are interpreted to be a contact layer between the Kebo-Butak's volcanic rocks and the younger formation. Figure 4 illustrates the lithologic composition of the northern Baturagung Range.

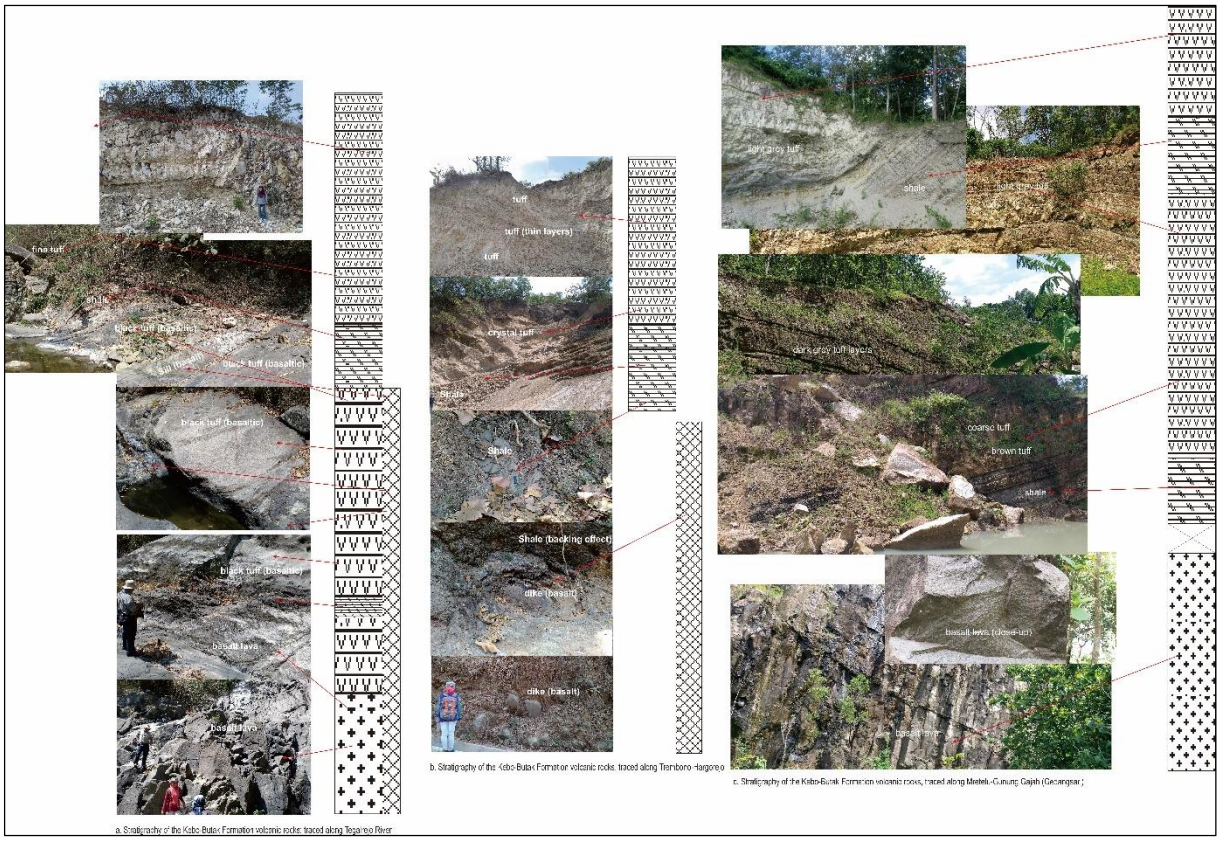

Fig 4. Stratigraphic sections of the Kebo-Butak Formation volcanic rocks, traced at Tegalrejo, Hargomulyo, and Gunung Gajah (northern slope of Baturagung Range).

Thick beds and layers of pumice-rich lapillistone and tuff in hundreds of meters cover the Kebo-Butak volcanic formation. Older publications called them to be the Semilir Formation. The sections across the Gunung Butak and Gunung Semilir (in the Gunung Wayang field complex; IH, Fig. 3) measured >200 m thickness of massive lapillistone and tuff. Cross lamination and cross-beds of tuff with pumice fragments in white color are exposed at Semin (GF, Fig. 3)), while the beds in yellowish color are exposed at Berbah (BK, Fig. 3). Massive beds of light grey pumice-rich lapillistone in very thick layers are exposed at Gunung Bangkel (near Berbah), while the white color in various structures (massive layers of >6m, layering @20-40 cm, thin layering of 5-10cm, and laminations) are exposed at Semilir (northern Nglanggeran) (JG, Fig. 3). The massive beds of dark grey pumice-rich lapillistone with glass and lithic fragments are exposed at Prambanan and Dahromo-Sindet (Jetis, Bantul). A thick layer of breccia with dacite, dense pumice, andesite, and basalt fragments grounded in the tuff matrix is exposed at Plencing and Panggung (near Semin). Some very angular chert fragments within 5-10 cm in diameter are often found in the deposits. It is poorly sorted, open fabric, and mostly very angular. This deposit is usually below the thick bed's lapillistone. The collected data inform the different colors of the lapillistone and tuff within the Semilir Formation. It tends to be different in composition and sources.

The wide distribution of the deposits and based on the reported publication before, the thickness of the pumice-rich tuff and lapillistone can reach more than 700 m. Stratigraphically, even there are different colors, structures, and compositions, mostly consisting of thick beds of lapillistone, layers or cross-beds of intersecting lapillistone and tuff, and finely covered by thin layers and laminations of fine tuff (Fig. 5). That's why these volcanic deposits often

described as volcanic turbidity currents mechanism (RAHMAD et al., 2017), (Patria et al., n.d.), (Chen et al., 2017), (Ardine et al., 2022).

Layers of crystal-rich sandstone with glasses and coral fragments are covering the Semilir's volcanic formation exposed at Semin (GF, Fig 3). Other outcrops show the sandstone layers intersecting with the brown sandstone exposed at Pengkok-Semoyo and Srumbung (Segoroyoso) (GL, GF, and GD, Fig.3), while some others present the sandstone with lignite exposed at Ngalang River (near Gedangsari) (GF, Fig. 3). Yellowish-light grey, poor sorting with small grains of embedded shells characterized those sediments. Above them are layers of ~2.6 m @ 10-20 cm calcareous sandstone with foram fossils as depicted in Figure 5. The sediments that are exposed near Ngrancahan (Pengkok, Patuk District; GL, Fig. 3), Wonolegi (near Gunung Ireng), Pucung (near Segoroyoso: AB, Fig 3) have a thickness of ~10 m, overlaying the crystal-rich sandstone. The foram fossils in it are *Globoquadrina altispira*, *Globigerinoides sicanus*, *Globigerinoides transitaria*, *Globigerinoides sacculiferus*, *Globigerinoides subquadratus*, *Globorotalia siakensis*, *Globorotalia mayeri*, *Praeorbulina glomerosa*, and *Hestigereina praesiphonifera*, suggests an age of N8-N9 (lower Middle Miocene). Additionally, the presence of *Bolivins sp*, *Cibicides sp*, *Gyoridina sp*, *Nodosaria sp*, and *Amphistegina sp* indicates an upper bathyal (~200-500 m depth). Stratigraphically, these sediments primarily constitute above the dacitic Semilir Formation and are not correlated with the Oyo Formation which is notably having an age of upper Middle Miocene.

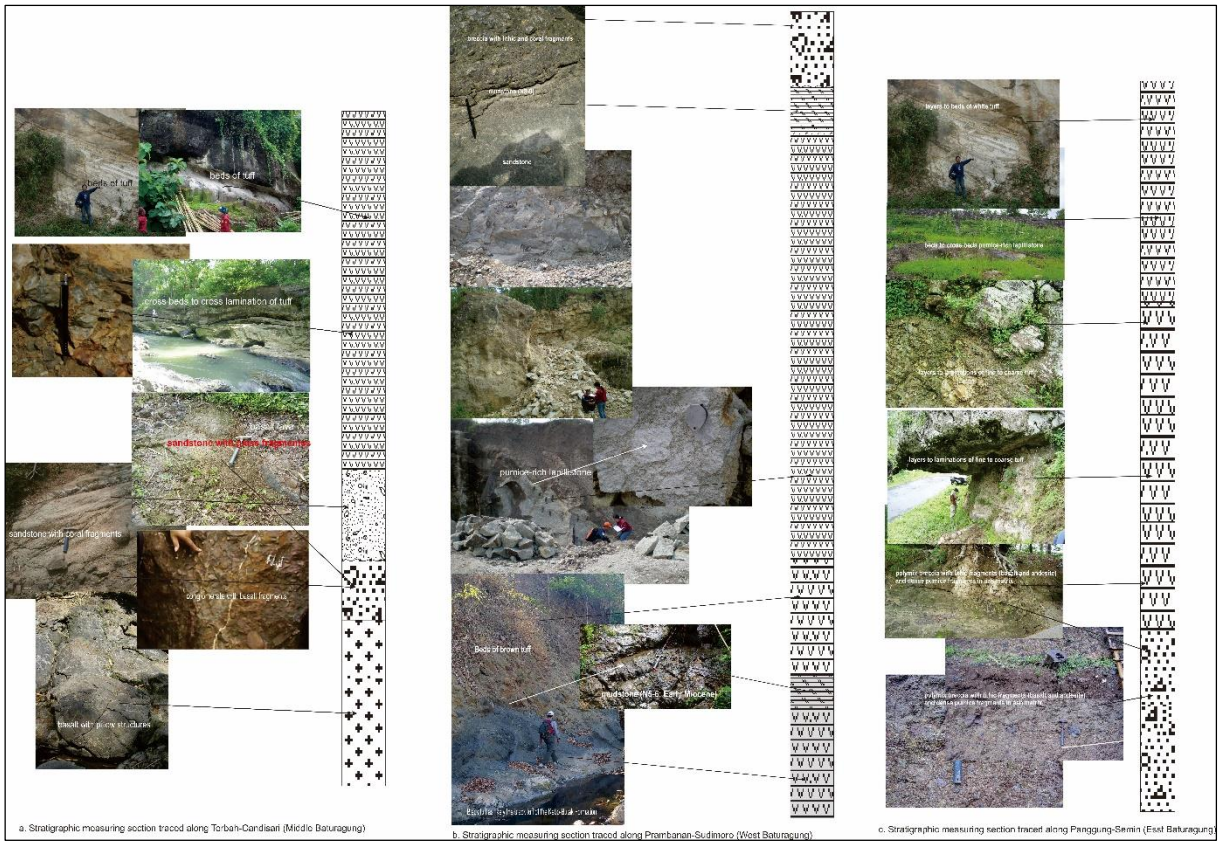

Fig 5. Stratigraphic sections of the Semilir Formation volcanic rocks traced at Terbah-Candisari (a), Prambanan-Sudimoro (c), dan Panggung-Semin (c).

Sections across the Gunung Nglanggeran's and Gunung Ireng's domes trending northeast-southwest (HCL, Fig. 3) show reddish pyroxene-rich basaltic lava (with augite, labradorite, and a small amount of olivine). Unconformity above the basaltic rocks are andesitic lava, agglomerate, breccia, and tuff. Those are massive, light grey to black (by oxidization), rich in pyroxene (aegirine) at Gunung Ireng but rich in hornblende at Gunung Nglanggeran. Generally, those volcanic rocks can be found in repeated layers of about 500-700 m total thickness. The dikes are often locally and associated with lava, blocky lava, agglomerate, and brown lapilli-tuff. Light grey crystal-rich calcareous sandstone (20-30cm thickness) containing lithic fragments in small sizes, and calcareous sandstone (~10 cm thickness) containing *Gq. altispira, Gs. sicanus, Gs. transitaria, Gs. sacculiferus, Gs. subquadratus, Gt. siakensis, Gt. mayeri, Praeorbulina glomerosa, and Hestigereina praesiphonifera* correlated to the Middle Miocene (N 8-9) are covering the volcanic rocks at Ngalang River. The same deposits exposed at the lower slope of Gunung Ireng have an age of Upper Early Miocene (N6-8) and Middle Miocene (N8-9). The sedimentary rocks consist of intersectinng calcareous sandstone and calcarenite of the Oyo Formation exposed at Beji (east of Gunung Ireng) are containing *Orbulina bilobata*, *Gs. altiaperturus*, *Gs. trilobus*, *Orbulina universa* dan *Sph. subdehischens* giving an age of N13 (Middle Miocene). According to (Smyth et al., 2008) the Semilir and Nglanggeran Formations's volcanic rocks are in an average of 20-19 Ma (Early Miocene), that possibly deposited in a short period. Notably, these volcanic rocks of the Nglanggeran Formation are having two sequences that consist of the basaltic volcanic rocks (the older) and the andesitic volcanic rocks (the younger).

Other sedimentary rocks that consist of thin layers of calcareous sandstone contain planktic forams of *Orbulina bilobata*, *Globorotalia altiaperturus*, *Globorotalia trilobus*, *Orbulina universa*, and *Sphaeroidinella subdehiscens*

indicate an age of N13 (the upper Middle Miocene) and benthic forams of *Eugrella sp* and *Eponides antilarum*, suggesting the middle Neritic zone (ranging from 30 to 150 meters below sea level) are exposed at southeastern Wonolegi. Calcarenite above the calcareous sandstone exposed at eastern Wonolegi contain *Globigerina praebulloides*, *Globorotalia immaturus*, *Sphaeroidinella subdehiscens*, *Orbulina bilobata*, *Globorotalia nephenthes*, and *Globigerina obessa*. These specimens indicate an age of N14-19 (the Upper Miocene to Early Pliocene). Benthic foraminifera that consist of *Cibicides sp*. suggests 30 to 100 meters water depth.

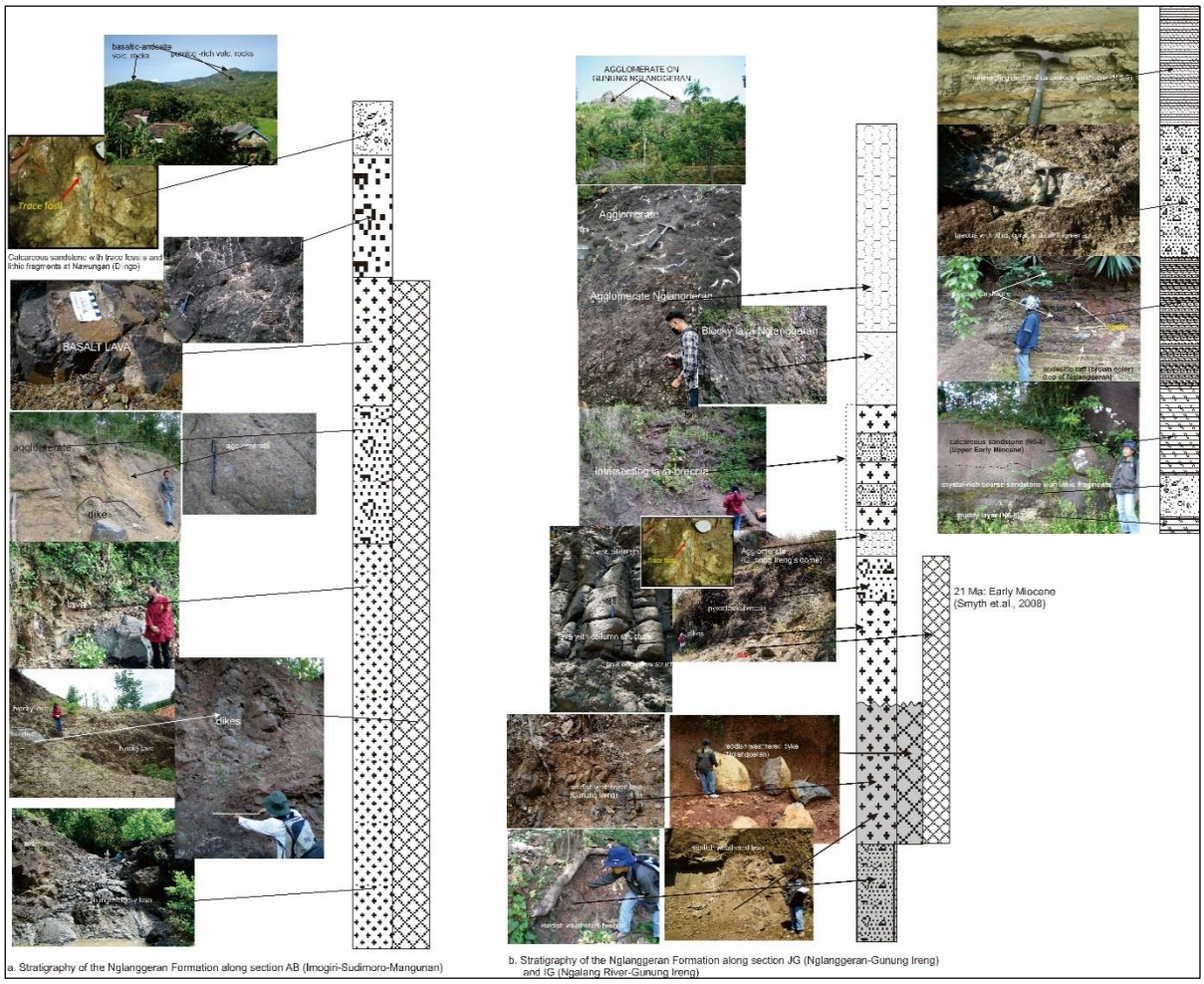

Fig 6. Sections trending northeast-southwest across Sudimoro (Imogiri)-Mangunan (Dlingo) (a) and Gunung Nglanggeran-Gunung Ireng (b). Those consist of basaltic (section of AB, see Fig.3) and andesitic volcanic rocks (sections of JG and IG, see Fig. 3)

4.2. Petrology

4.2.1. Thin Sections

The previous chapter describes the stratigraphy of the Kebo-Butak (oldest), Semilir (older), and Nglanggeran (younger) Formations that compose the Baturagung Range. Figure 7 shows details of the thin sections of the Kebo-Butak Formation. Normally, there are clastic and coherent volcanic rocks. The clastic consists of black tuff, brown tuff, and breccia, as described by the stratigraphic chapter above. The black tuff unit is dark (black) color, well sorted, and composed of pyroxene and basaltic glass (ash; Fig. 7.a) in dust to ash grain sizes with glass matrix. The crystals are mostly very angular, but the ash and dust are mostly rounded. The fine grain's black tuff exposed at Tegalrejo is well sorted and composed of glasses only (Fig. 7c), sometimes containing coral fragments, so it's described as sandstone with granule fragments (sedimentary rock) by the previous publications (Surono, 2009), (Chen et al., 2017), (Akmaluddin et al., 2024). The brown tuff that is exposed at Karangtengah is found in thick layering (more than 5-8 m for each layer). It's poorly sorted, containing lithic fragments and crystals of pyroxene and ash (glass) in ash sizes (Fig. 7.d). The basalt lava can be found as a basalt layer, with pillow structures, intersecting with black tuff, and column structures. Basalt lava with pillow structures exposed at Berbah is characterized by porphyritic texture, composed of plagioclase (bytownite), Clinopyroxene, glass, and microcrystals of clinopyroxene and olivine; mostly anhedral (Fig. 7.b). The basalt with column structures exposed at Karangtengah and Gunung Ireng is characterized by vesicular-scoriaceous, porphyritic, and composed of plagioclase (labradorite), clino-pyroxene and litle bit small grains of microcrystal olivine (Fig. 7.e). The basalt intersecting with the black tuff shows scoriaceous to vesicular, porphyritic to vitric, composed of clinopyroxene (augite), plagioclase (bytownite), and the small grains of olivine as microcrystal together with the glasses to be the groundmass. The light grey tuff of the Kebo-Butak Formation is found as described in the stratigraphic section above, with no thin section in it caused by the very fine and very loose, even that's deeply altered. Lithic tuff with black color exposed at Tegalrejo is massive, composed of basalt lithic in lapilli sizes, lithic in ash sizes, and glass matrix, poorly sorted, angular shapes, and open fabric (Fig. 7f). Based on thin section observation, the Kebo-Butak Formation is also composed of many types with different properties of volcanic

rocks. The major elements are composed of SiO_2 51-55.7% weight, Fe_2O_3 10-11% weight, CaO ~7-8% weight, MgO ~5-6% weight, Na_2O ~3-3.5% weight, low K (< 1% weight), and higher TiO_2 (0.7-1.6% weight).

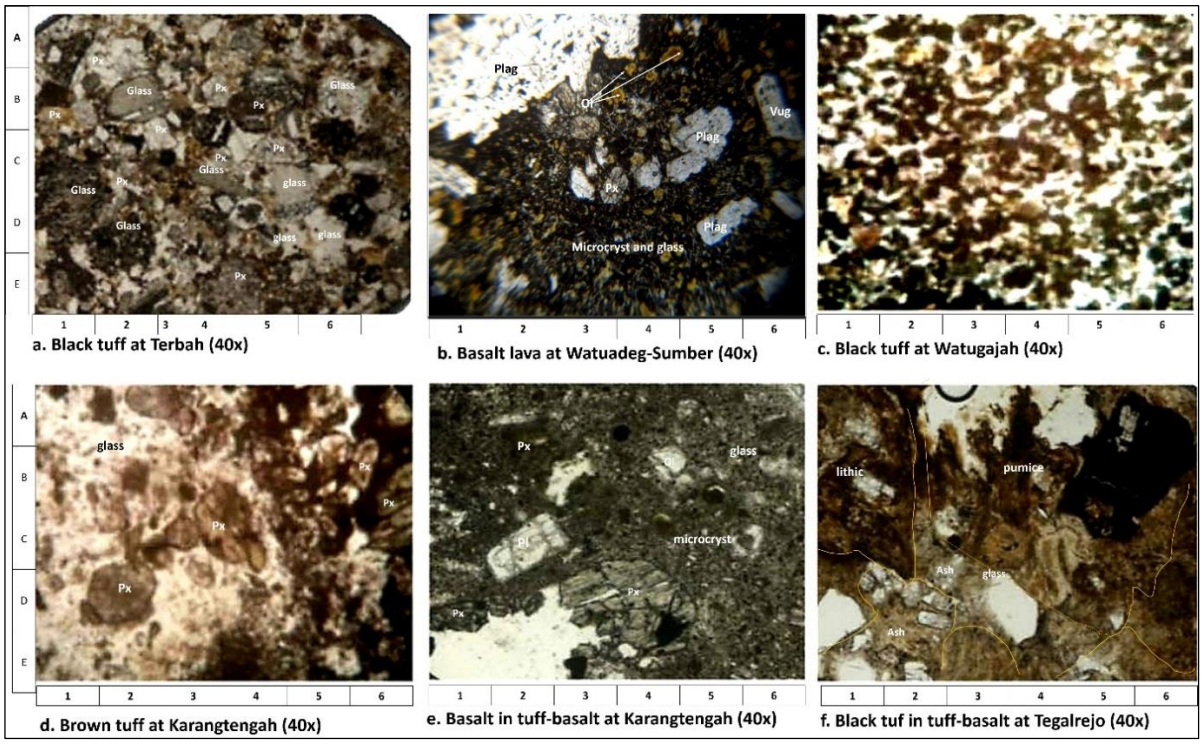

Fig. 7. Photomicrographs of the Kebo-Butak Formation's volcanic rocks exposed at the Baturagung Range

The Semilir Formation which is composed of clastic volcanic rocks (pumice-rich and tuff), is deeply fragmented. The pumice-rich volcanic rocks are massive to beds. As a megascopic observation, there are dark grey pumice rich with basalt glass (exposed at Dahromo Jetis-Imogiri; west), light grey pumice-rich (exposed at Ngelo-Prambanan-Berbah; middle), and yellowish grey pumice-rich (exposed at Semilir and its surrounding; east) volcanic rocks. The thin sections of the dark grey pumice-rich are rounded pumices with irregular shapes, dark grey ash matrix, medium-well sorted, in massive structures (Fig. 8.a). The very thick beds (>10 m for each bed) are well sorted, rich in basalt glasses, angular to rounded fragments of glass and lithic (Fig. 8b). The laminated to layered dark grey tuff, there are poorly sorted with basaltic glass and vitric ash (Fig. 8c). The thin sections of the light grey volcanic rocks of the middle part of Baturagung Range is the presence of small ashes and twig fragments within the light grey vitric matrix (Fig. 8d). The massive pumice-rich volc. rocks consist of subangular to rounded ~4mm dacitic glass fragments (with feldspar and quartz), in the ashy matrix, in well sorted (Fig.8e). The layered very fine volcanic rocks exposed in the complex palace of Ratu Boko and Gunung Bangkel at Prambanan are characterized by poorly sorted, consist of angular dacitic lithic glass fragments within vitric ash matrix (Fig. 8.f). The yellowish-grey volcanic rocks exposed at the east of the Baturagung Range consist of yellowish ashes with feldspars and fine grains of quarts (Fig. 8g-h), while the pumice-rich volc. rocks are subangular to rounded fragments consisting of light glasses in well-sorted (Fig. 8i). Based on the megascopic and microscopic observations, the Semilir Formation is composed of varying pumice-rich volcanic rocks.

The Nglanggeran Formation is notably composed of andesitic fragmented and coherent volcanic rocks, as described in chapter Stratigraphy above. Most of the Nglanggeran Formation volcanic rocks are composed of clinopyroxene as the mafic minerals. The thin sections of the pyroxene-rich andesitic vol. rocks exposed at Dlingo (west Baturagung) are vesicular, porphyritic with augite (~25%) and labradorite phenocrysts, within the dark color of glass as the groundmass (Fig. 9a). For a while, microcrystals are consisting the thin section of pyroxene-rich andesite exposed at Candisari (Prambanan) (Fig. 9b). Those are vesicular-scoriaseous, porphyritic with the phenocrysts are labradorite and augite (~20%). Pyroxene-rich andesitic volcanic rocks exposed at Giriloyo consist of augite and aegirine (~30%), a little bit olivines, labradorites, and glass groundmass (Fig. 9c). The thin sections of the Nglanggeran Formation volc. rocks exposed at the Middle Baturagung have bigger crystals such as shown in Fig. 9d-f. Those are vesicular, porphyritic with aegirine as the mafic phenocrysts (~35%) and andesine-labradorite phenocryst in the glass groundmass (Fig. 9d), while the samples taken in Gunung Ireng contain augite (~30%) as the mafic phenocrysts (Fig. 9e), and older andesite lava with the reddish color exposed at the lower slope of Gunung Ireng consists of aegirine with euhedral shape (~35%) and labradorite in dark color of glass groundmass (Fig. 9f). The andesitic volc. rocks exposed at Nglanggeran consist of pyroxene and hornblende as the phenocrysts (~35%) with anhedral shapes, vesicular, porphyritic within the groundmass consisting of glass and microcryst. As described above, the volcanic rocks of the Nglanggeran Formation are found in many types. The same properties that unify them are their physical forms, which consist of lava, breccia, and agglomerate, even in the local sections are andesitic brown tuff or the lithic tuff.

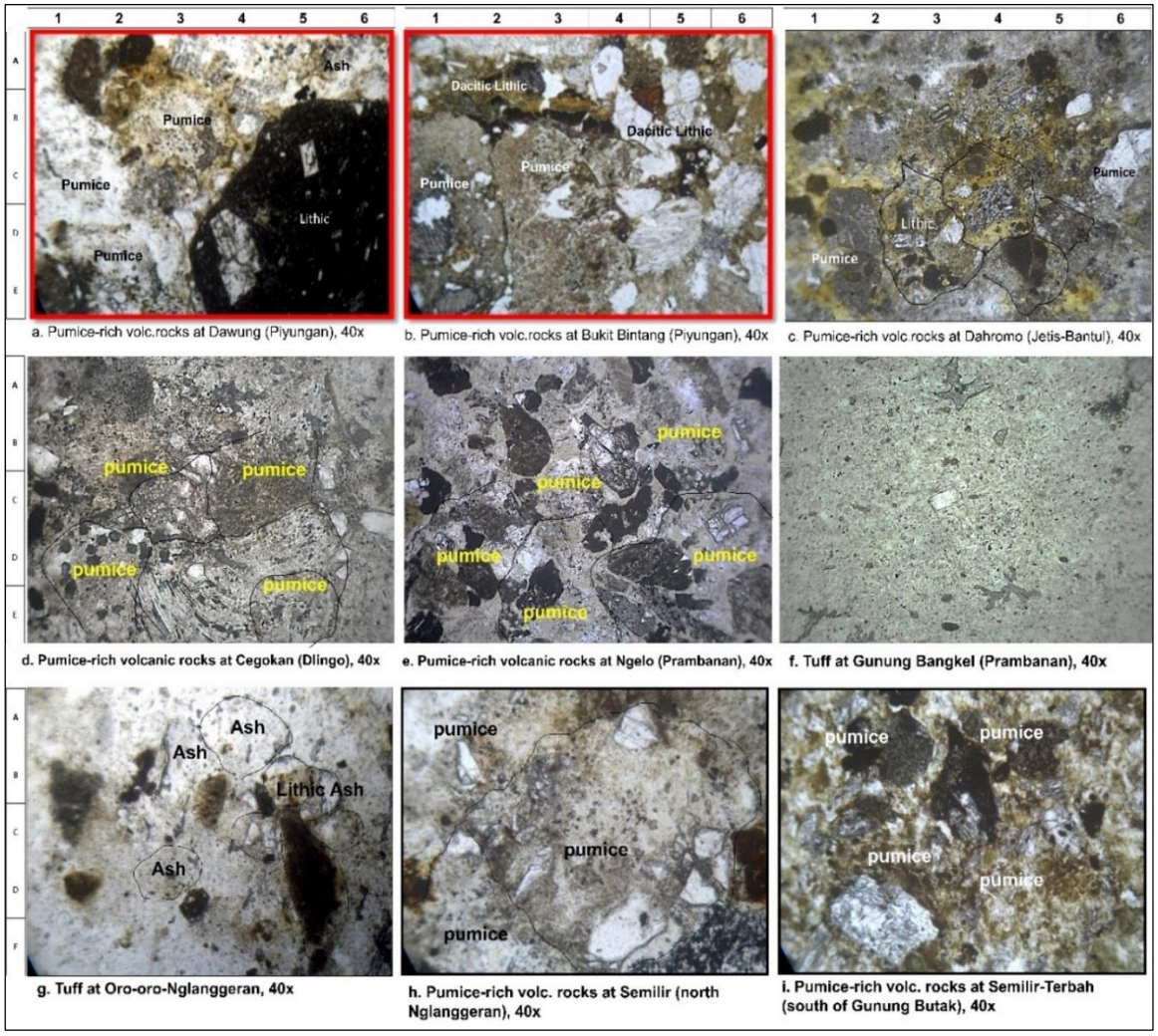

Fig. 8. Photomicrographs of the Semilir Formation's volcanic rocks exposed at Baturagung Range

4.2.2 Major Elements

Table 2 represents the major elements of the Baturagung Range's volcanic rocks. As described by stratigraphy and thin sections, also according to the previous publications the volcanic rocks are divided into 3 formations (Rahardjo et al., 1995b), (Surono et al., 1992); the Kebo-Butak, the Semilir, and the Nglanggeran Formations.

As listed in Table 2, the Kebo-Butak Formation's vulc. rocks consist of ~51-55% wt SiO_2, ~10-11% wt Fe_2O_3, ~4.5-6% wt MgO, and ~7-8% wt CaO that represent the presence of the mafic minerals. Those samples are also containing ~3-3.85% wt Na_2O, ~0.5-1% wt K_2O, and ~15-17% wt Al_2O_3. Some of them have more than 1% wt TiO_2 and ~2% wt of the loss of ignition (LOI) for the tuff and lapillistone samples. These data show different values for the major elements, which represent the optical properties so that those are different sub-volcanic rock formations. The higher values of iron (Fe_2O_3) and calcium oxide (CaO) in the basalt lava may be attributed to the higher presence of clinopyroxene (augite). The elevated Fe_2O_3 (~10-11%) and TiO_2 (~0.8%) indicate substantial quantities of titanites, which are discernible in thin sections exhibiting intergrowths with clinopyroxene (augite).

The major elements of the Semilir Formation's volcanic rocks are characterized by a SiO_2 composition range of 57-60%, Al_2O_3 at 18%, a CaO range of 5-7%, and a Fe_2O_3 range of 6-8%. The optical properties indicate that this volcaniclastic materials contain feldspar and quartz, but the maximum SiO_2 is only ~60%. Another interesting data point is that this dacitic rock contains Na_2O at only 3.4-4%, which tends to be more andesitic, with a very high degree of fragmentation. Similarly, the K_2O is relatively low to medium, ranging from 0.5-0.6%.

The major elements contained in the andesite are 56.5-57% wt of SiO_2, ~18% wt of Al_2O_3, ~7% wt of CaO, ~3.9% wt of Na_2O, and ~8% wt of Fe_2O_3. The higher content of sodium (Na_2O) and aluminum oxide (Al_2O_3) indicates the prevalence of andesine (a sodium-calcium plagioclase mineral). These rocks also contain medium and small grains of aegirine, a calcium-iron-sodium pyroxene, and an increased amount of glass in comparison to the basaltic volcanic rocks (Fig. 9. e-f).

The variation in major elemental composition concerning SiO_2 is employed to delineate the different magma sources, as depicted in Fig. 10. This includes the elements Al_2O_3, K_2O, Na_2O, CaO, MgO, Fe_2O_3, P_2O_5 and TiO_2 concerning SiO_2 for comparative purposes, and also for total K_2O+Na_2O versus total CaO+MgO and total CaO+Fe_2O_3. Notably, a decrease in Al_2O_3 indicates a higher abundance of plagioclase in andesite. The SiO_2 increase in andesite is not accompanied by significant variations in K_2O and Na_2O. This indicates that the trends do not apply to magma evolution in the same volcano, but may be due to differences in volcanic sources that produce different rock sequences.

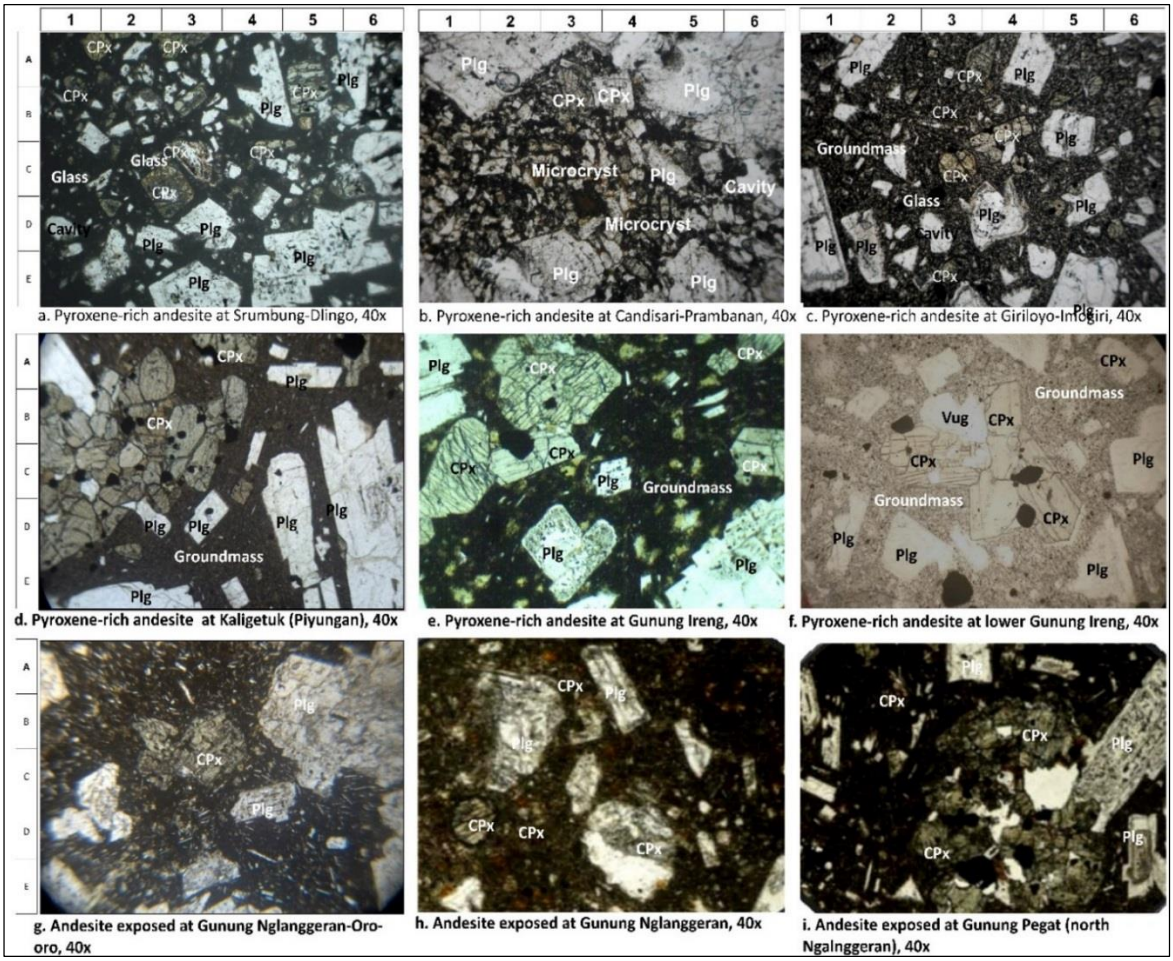

Fig. 9. Photomicrographghes of the Nglanggeran Formation's volcanic rocks exposed at Baturagung Range

The Harker's Diagram (Fig. 10) finds positive trends for the plots of Al_2O_3, Na_2O, and P_2O_5 concerning SiO_2 in the opposite, the negative trends are found in the plots of K_2O, CaO, MgO, Fe_2O_3, and TiO_2 (Fig. 10). The negative trend for the plot K_2O versus SiO_2 is an anomaly, that it can mean as different source of magmatism not for magmatic evolution. The rise in SiO_2 corresponds with a decline in CaO, MgO, TiO_2, MnO, and P_2O_5. Negative trends observed in the plots for Fe_2O_3 and MgO indicate the presence of significant amounts of clinopyroxene (augite), and the negative trends for MgO and Fe_2O_3 suggest the occurrence of olivine. Positive trends in Al_2O_3, Na_2O, and CaO correspond to the presence of labradorite and andesine in the andesite. Negative trends in the TiO_2 plot are likely related to the presence of lithophile minerals, possibly titanites in augite (Fig. 7-9), as previously proposed by (Grasso, 1968), (Niu et al., 2006), and (Mullen, 1983). This trend reflects the higher concentrations of Ti. Negative trends in the P_2O_5 plot are attributed to the presence of apatite, while the negative trends in the MnO plot correspond to the presence of manganite, although not in significant quantities, Mn^{2+} might replace Fe_2O_3 in andesite. It's noteworthy that the increase in Al_2O_3 for andesite does not exhibit a corresponding linear decrease in TiO_2. The TAS diagram as the plot of total Na_2O+K_2O vs. SiO_2 according to (Le Maitre et al., 2005) characterizes basalt, basaltic andesite, and andesite (Fig. 11).

Table 2. The Major elements of the Kebo-Butak Formation's volcanic rocks, the dacitic Semilir Formation's volcanic rocks, and the andesitic Nglanggeran Formation volcanic rocks are exposed at the Baturagung Range.

Major elements	*The Basaltic Kebo-Butak Formation's Volcanic Rocks*						*The Dacitic Semilir Formation's Volcanic Rocks*				*The Andesitic Nglanggeran Formation's volcanic rocks*			
	B.1 A	B.1 B	A.10	C.13 A	C.10	C11	A.11	A.12	A.13	A.14	B.20	B.21	B.22i	B.23
SiO_2	51.2	51.3	54.22	55.17	55.73	54.12	58.01	57.27	57.06	59.01	57.0	56.01	57.0	56.52
Al_2O_3	14.9	15.1	17.24	17.21	17.17	17.01	18.7	18.0	18.02	18.0	18.02	18.02	18.1	18.31
K_2O	0.95	0.93	0.54	0.54	0.55	0.53	0.6	0.57	0.61	0.66	0.55	0.55	0.45	0.56
Na_2O	3.38	3.35	3.03	3.73	3.85	3.53	4.01	3.79	3.67	4.19	4.01	3.79	4.0	3.72
CaO	8.22	8.28	7.82	6.72	7.18	7.87	5.82	6.6	6.97	5.11	7.02	7.01	6.54	7.33
MgO	5.97	6.12	5.02	4.9	4.46	5.51	5.15	4.8	4.68	4.18	6.06	5.12	5.13	4.18
MnO	0.18	0.19	0.12	0.12	0.12	0.13	0.08	0.09	0.098	0.07	0.07	0.11	0.07	0.11
TiO_2	1.61	1.6	0.8	0.77	0.79	0.82	0.7	0.71	0.76	0.7	0.77	0.75	0.75	0.73
Fe_2O_3	11.1	11.1	10.9	10.7	9.84	10.2	6.12	7.92	7.82	6.01	6.6	7.92	8.04	8.23
P_2O_5	0.15	0.15	0.27	0.22	0.25	0.26	0.24	0.24	0.27	0.26	0.20	0.22	0.18	0.25
LOI	2.34	1.88	0.074	0.08	0.08	0.08	0.47	0.02	0.05	0.81	0.01	0.50	0.06	0.06
Total	100.0	100.0	100.0	100.0	100.0	100.0	100.0	99.99	99.99	99.18	100.0	100.0	99.9	99.9

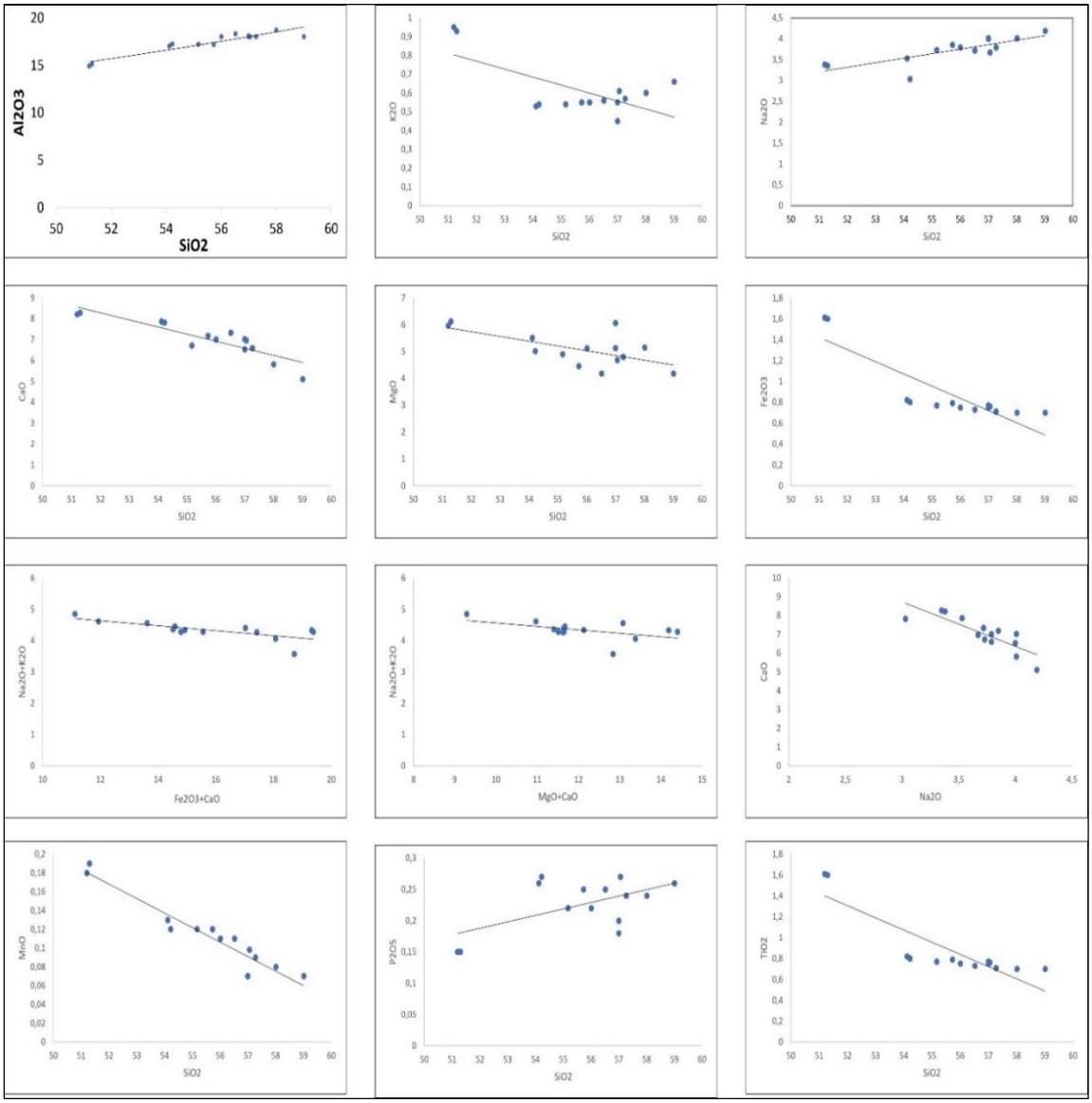

Fig 10. The Harker's variation diagram (according to (Pearce, 1996) of the plot silica to Al_2O_3, K_2O, Na_2O, CaO, MgO, TiO_2, Fe_2O_3, MnO, and P_2O_5

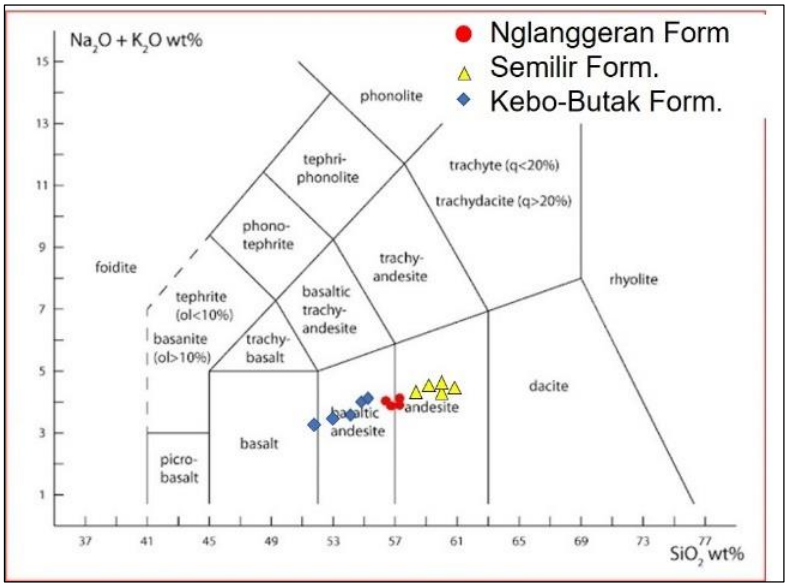

Fig 11. The TAS Diagram shows basaltic andesitic volcanic rocks for the pyroxene-rich andesitic volcanic rocks as the older and andesitic volcanic rocks for the younger (following Le Maitre *et al*., 2005)

The plots K_2O vs. SiO_2 and the AFM Diagram (Figure 12. a-b) suggest that the volcanic rocks are low to medium-K Calc-alkaline series.

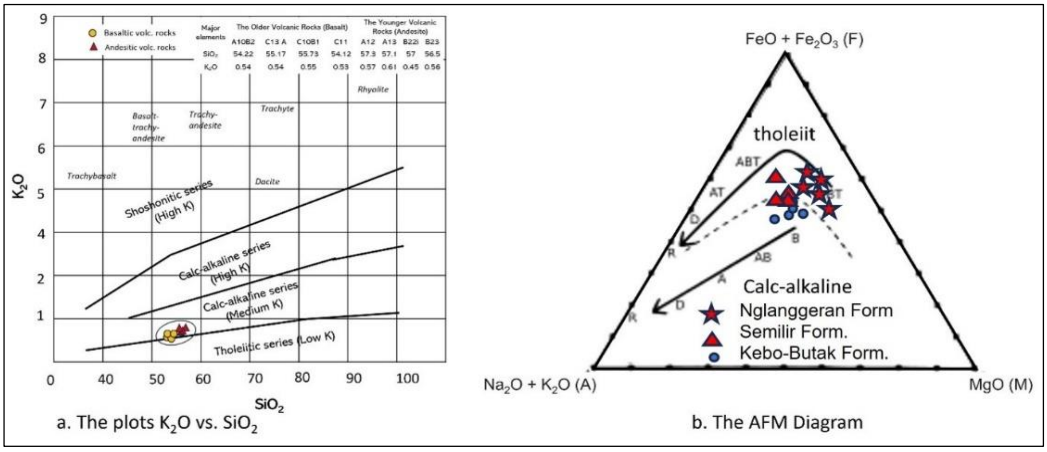

Fig 12. Volcanic rocks classification (Peccerillo and Taylor, 1976) of plot K_2O and SiO_2 suggests that both volcanic rocks are medium K Calc-alkaline series.

5. Table 3. Trace elements in the Baturagung Range's Volcanic Rocks (in part per million).

No. Sample	A10B2	C13 A	C10B1	C11	A12	A13	B22i	B23
Rock Types	Basalt	Basalt	Basalt	Basalt	Andesite	Andesite	Andesite	Andesite
S	0.01	0.01	0.01	0.01	0.01	0.01	0.01	0.01
Cr_2O_3	<0.005	<0.005	<0.005	<0.005	<0.005	<0.005	<0.005	<0.005
Al	97,600	104,000	101,000	94,000	101,000	101,100	104,000	104,000
Ca	69,000	75,600	72,300	73,200	46,600	45,700	46,700	39,500
Cr	28	37	36	36	6	6	6	6
Cu	298	140	113	170	16	15	17	13
Fe_pct	7.5	6.99	7.2	7.29	5.8	5.87	5.88	4.99
K	14,700	12,400	13,800	14,200	14,300	13,700	14,300	12,700
Mg	25,800	25,900	27,300	27,300	13,200	12,100	13,500	14,800
Mn	1,160	1,160	1,210	1,210	1,040	1,280	1,220	1,170
Na	20,700	20,000	21,200	21,100	25,800	25,800	25,000	25,700
Ni	21	25	27	24	6	5	6	4
P	930	840	910	900	1160	1330	1320	1320
S	<50	<50	<50	<50	50	50	50	50
Sc	24	25	25	25	13	12	13	10
Ti	4830	4900	4940	4940	4540	4360	4400	4340
V	296	262	302	302	141	92	111	93
Zn	96	92	91	91	99	103	104	106
Ag	0.1	0.1	<0.1	0.1	0.1	0.1	0.1	0.1
As	3	2	2	2.6	4	4	3.6	3.4
Ba	571	574	577	576	380	380	385	384
Be	0.6	0.6	0.6	0.6	1.1	1.1	1.3	1.4
Bi	0.05	0.05	0.05	0.05	<0.05	<0.05	<0.05	<0.05
Cd	0.08	0.09	0.09	0.9	0.18	0.19	0.18	0.19
Co	30	28	29	29	12	13	12	8
Cs	2	2.4	2.1	2.2	2.8	2.8	2.78	2.78
Ga	19.9	20.3	20.3	20.5	22.7	22.7	22.9	23.2
Ge	1.6	1.6	1.7	1.6	1.9	1.9	1.8	1.9
Hf	1.7	1.9	1.8	1.8	3.5	4.7	4.1	4.7
In	0,05	<0,05	0,05	<0,05	0.06	0.06	0.06	0.06
Li	11.7	11.2	11.4	11	20.2	21.9	22	27.4
Mo	0.8	0.6	0.7	0.7	1.1	1.1	1.2	1.1
Nb	2.8	2.7	2.7	2.8	6.5	6.8	7.3	7.9
Pb	18	18	18	17	13	12	13	13
Rb	23.7	22.2	23.1	23.6	22.7	22.6	22.8	22.8
Re	<0.05	<0.05	<0.05	<0.05	<0.05	<0.05	<0.05	<0.05
Sb	0.2	0.2	0.1	0.2	0.2	0.2	0.2	0.2
Se	<1	<1	<1	<1	<1	<1	<1	<1
Sn	0.7	0.7	0.7	0.7	1.5	1.45	1.1	1.35
Sr	549	602	593	549	498	499	485	485
Ta	1.15	1.00	0.99	0.98	0.78	0.75	0.77	0.76
Te	<0.1	<0.1	<0.1	<0.1	<0.1	<0.1	<0.1	<0.1
Th	5.79	5.64	5.74	5.74	8.77	9.57	8.66	7.98
Tl	0.06	0.06	0.08	0.07	0.22	0.20	0.18	0.22
U	1.01	0.95	0.80	1.68	1.92	1.88	1.78	1.92
W	0.7	0.7	0.5	0.6	1.00	1.12	0.99	1.01
Zr	53.3	58.2	59.2	59.3	129	171	167	155

5.1.1. Trace Elements

The trace elements are applied only in the basalt lava of the Kebo-Butak Formation and the andesite lava in the Nglanggeran Formation, as presented in Table 3. It shows higher concentrations of mobile elements, such as Sr (~480 ppm in basalt, increasing to ~602 ppm in andesite, as well as medium amounts of Rb (22.2-23.7 ppm) and La (12-21 ppm). It's important to note that Sr is compatible with plagioclase, as illustrated in Fig. 8. a-f, where plagioclases are predominant in phenocrysts and groundmass. The presence of medium Rb and La indicates a low-K Calc-alkaline series and medium-K Calc-alkaline series (Fig. 10).

The Barium (Ba) falls within ~380 ppm in andesite and 571-577 ppm in basalt, Thorium (Th) is detected in moderate amounts (~5.74 ppm in basalt and ~8.77 ppm in andesite), and Cerium (Ce) of ~25 ppm in basalt and ~40 ppm in andesite. In contrast, immobile trace elements like Nb (2.7 ppm in basalt and 6.5-7.9 ppm in andesite), Zr (53-59 ppm in basalt and 129-171 ppm in andesite), and P (840 ppm in basalt and ~1300 ppm in andesite) exhibit higher concentrations. Medium levels are observed in Ti (4400-4900 ppm), and Vanadium (V) is notably elevated (92 ppm in andesite and 302 ppm in basalt). Ni and Cr concentrations are noteworthy; low Ni (~5 ppm) and Cr (<34 ppm) in andesite suggest partial melting, while higher Cr (~35 ppm) and Ni (~26 ppm) in basaltic andesite imply magma mixing and mingling. To summarize Tables 3-4 categorize the elements into three groups: MRFE (mantle rock-forming elements) comprising Si, Al, Cr, Na, Mg, Fe, Cu, Zn, Co, and Ni; LILE (mobile elements) encompassing Eu, Pb, Sr, Ba, K, Rb, and Cs; and HFSE (immobile elements) consisting of P, Nb, Ta, W, Ti, Zr, Pb, Th, U, Hf, Y, Lu, Eu, and La.

5.1.2 Rare Earth Elements

Table 4 lists the rare earth elements (REE) concentrated in basaltic and andesitic volcanic rocks of the Kebo-Butak and Nglanggeran Formations. They are divided into light REE (LREE) in an amount of ~69% and heavy REE (HREE) in ~31%. As described in the Periodic System, LREE refers to the first 7 elements in the REE group, from Lanthanum (La) to Gadolinium (Gd). As follows, (Sheth et al., 2002) argue that LREE is typically more abundant than HREE in calc-alkaline volcanic rocks, which tend to be more compatible with minerals formed under higher temperatures and lower pressure conditions; in this case, plagioclase and apatite. As a result, they are often concentrated in these minerals during volcanic processes; the higher percentage of LREE indicates the rocks were formed in magmatic environments with partial melting. This can be associated with various geological settings of the subduction zone. As a comparison, the HREE is less compatible with volcanic common rock-forming minerals and is interpreted as a remnant of the residual melt after the crystallization of primary minerals. The distribution of LREE and HREE provides partial melting within plate boundaries of the active continental margin.

Incompatible to compatible multi-trace elements diagram normalized to Primitive Mantle, according to (La Flèche, Camire, and Jenner, 1998) (Fig. 13. a), shows the volcanic rocks of the study area are depleted in Tm and Lu, slightly enriched for the elements of decreasing compatibility, and mostly moderately to strongly metazomatized for the elements of Ba, P, Sr, Ti, and Y. The Chondrite normalized for the REE concentrations in these rocks are compared and scaled relative to the composition of CI chondrite. Positive trends for certain REEs, specifically Ce, Gd, Zr, and Y, indicate higher concentrations of the REEs than in the CI chondrite reference; the higher specific REEs suggest enrichment. Negative trends are found in Pr, Nd, Sm, Eu, and Tb; suggesting any depletion that is less prominent in the mineral composition. The positive trends of Gd and Zr and the negative trends of Sm and Eu correlate with the higher presence of augite and the smaller amounts of plagioclase (a common feldspar mineral in a calc-alkaline volcanic rock). Eu is known for its unusual behavior; it has two valence states, Eu^{2+} and Eu^{3+} and it can be incorporated into different mineral phases.

Table 4. Rare earth elements contained in the Kebo-Butak and the Nglanggeran Formations of the Baturagung Range

No. Sample	***A10B2***	***C13 A***	***C10B1***	***C11***	***A12***	***A13***	***B22i***	***B23***	*Average*	*%*	*REE*	
Rock Types	Basalt	Basalt	Basalt	Basalt	Andesite	Andesite	Andesite	Andesite				
La	12.1	12.1	12.1	13.0	21.3	21.3	20.4	20.9	16.65	15	LREE=	69%
Ce	24.9	25.0	25.8	25.4	46.1	46.6	46.4	46.5	35.85	32		
Pr	2.9	2.94	3.05	3.04	5.23	5.25	5.23	5.27	4.11	4		
Nd	12.4	12.4	13	12.7	21.4	21.4	21.1	21.3	17	15		
Sm	3.1	3.1	3.2	3.2	4.7	4.6	4.6	4.8	3.91	3		
Eu	0.9	0.9	1.0	1.0	1.3	1.3	1.4	1.4	1.15	1	HREE=	31%
Gd	3.7	3.7	3.5	3.6	4.7	4.8	4.7	4.6	4.16	4		
Tb	0.46	0.45	0.47	0.46	0.64	0.63	0.66	0.64	0.55	0.5		
Dy	3.1	3.0	3.2	3.1	4.1	4.3	4.2	4.2	3.65	3		
Ho	0.6	0.6	0.6	0.6	0.8	0.8	0.8	0.8	0.7	1		
Er	1.7	1.7	1.7	1.7	2.4	2.6	2.4	2.6	2.1	2		
Tm	0.2	0.2	0.2	0.2	0.3	0.3	0.4	0.4	0.28	0,24		
Yb	1.7	1.6	1.7	1.7	1.79	2.3	2.7	2.18	1,96	2		
Lu	0.24	0.25	0.26	0.26	0.36	0.38	0.41	0.40	0,32	0,28		
Y	16.6	16.6	17.8	17.4	22.7	23.8	23.6	23.8	20,29	18		
dEu	**0.81**	**0.84**	**0.89**	**0.88**	**0.82**	**0.83**	**0.82**	**0.83**				

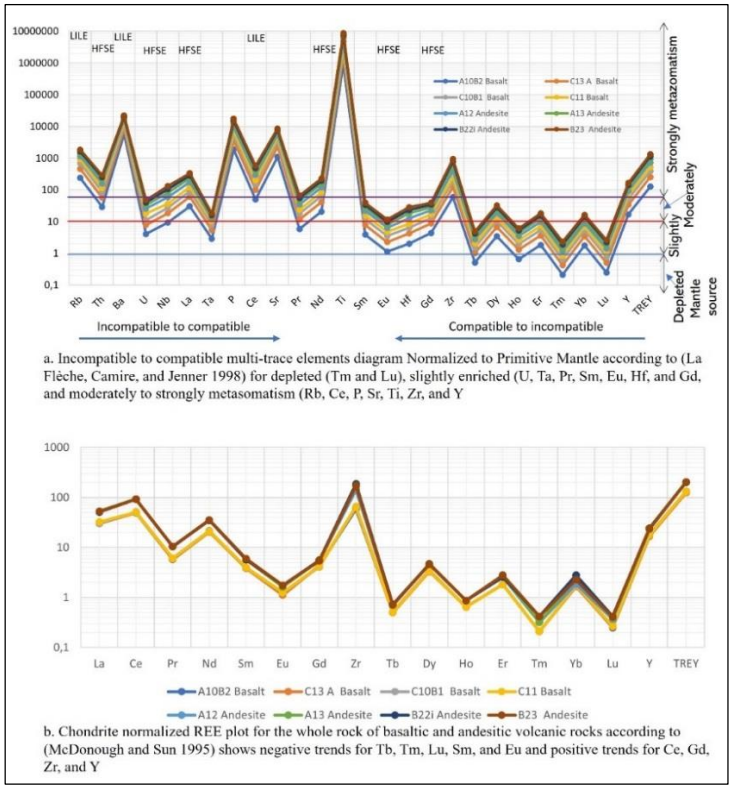

a. Incompatible to compatible multi-trace elements diagram Normalized to Primitive Mantle according to (La Flèche, Camire, and Jenner 1998) for depleted (Tm and Lu), slightly enriched (U, Ta, Pr, Sm, Eu, Hf, and Gd, and moderately to strongly metasomatism (Rb, Ce, P, Sr, Ti, Zr, and Y

b. Chondrite normalized REE plot for the whole rock of basaltic and andesitic volcanic rocks according to (McDonough and Sun 1995) shows negative trends for Tb, Tm, Lu, Sm, and Eu and positive trends for Ce, Gd, Zr, and Y

Figu 13. The incompatible to compatible multi-trace elements of the Kebo-Butak and the Nglanggeran Formations of the Baturagung Range's and the Chondrite normalized REE (McDonough and Sun, 1995).

Plot Nb/Zr vs. La/Yb (Figure 14) suggests a slightly enriched mantle source for the basaltic volcanic rocks under consideration. This enrichment indicates the magma source had higher concentrations of certain elements, possibly due to past geological processes. According to (Chen et al., 2021), Calc-alkaline basaltic andesite exhibits higher Cr and Ni levels compared to tholeiitic basaltic andesite, while bronzite andesite displays elevated MgO, Cr, and Ni in comparison to typical calc-alkaline andesite with a similar SiO_2 content. All these rock series are found a depletion in high field strength elements (HFSE) such as Nb and Ti; suggesting subduction-related arc magmas association. The high Zr/Y ratios observed in tholeiitic basalt resemble the compositions typically found in active continental margin magmas rather than island-arc magmas. The variations in HFSE, Ni, and Cr compositions across the different rock types suggest a progressive depletion or an increasing degree of partial melting in the mantle wedge source, with the sequence being tholeiite basalt (basaltic andesite)→calc-alkaline basaltic andesite

Plot Hf/Sm vs. TREY (Figure 15), according to La Fleche et al. (1998) as cited in (Godang et al., 2021), indicates that the basaltic volcanic rocks were metasomatized in a subduction zone, while the andesites had a strongly metasomatized in the hydrated mantle source. Plot TiO2 vs. Al2O3 (Figure 16), according to Müller and Groves (1993), suggests that the magma source was related to the plate mechanism.

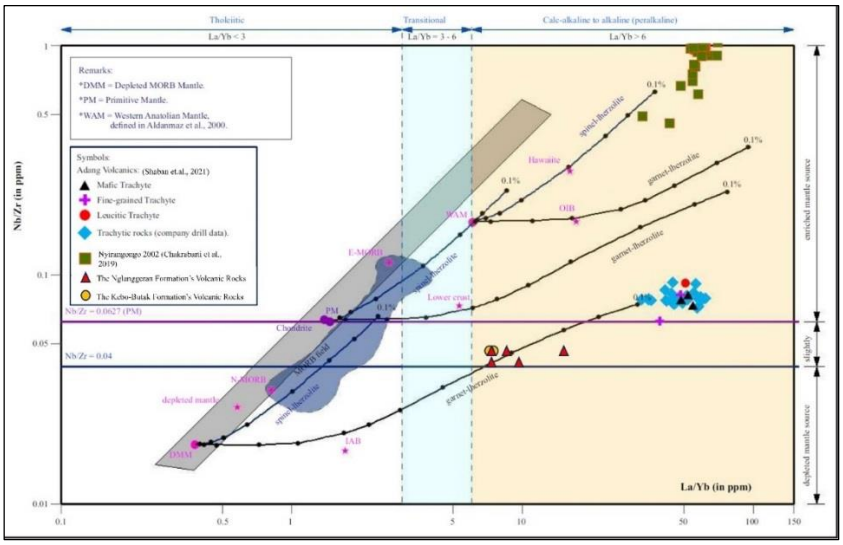

Fig 14. Plots Nb/Zr versus La/Yb show a slightly enriched mantle source with the comparations are Adang Volcano (Godang et al., 2021), Vulsini Volcanic Rocks (Nappi et al., 1998), madapitic lamproites (Mitchell et al., 1991), and the Nyiragongo volcanic rocks (Chakrabati et al., 2009).

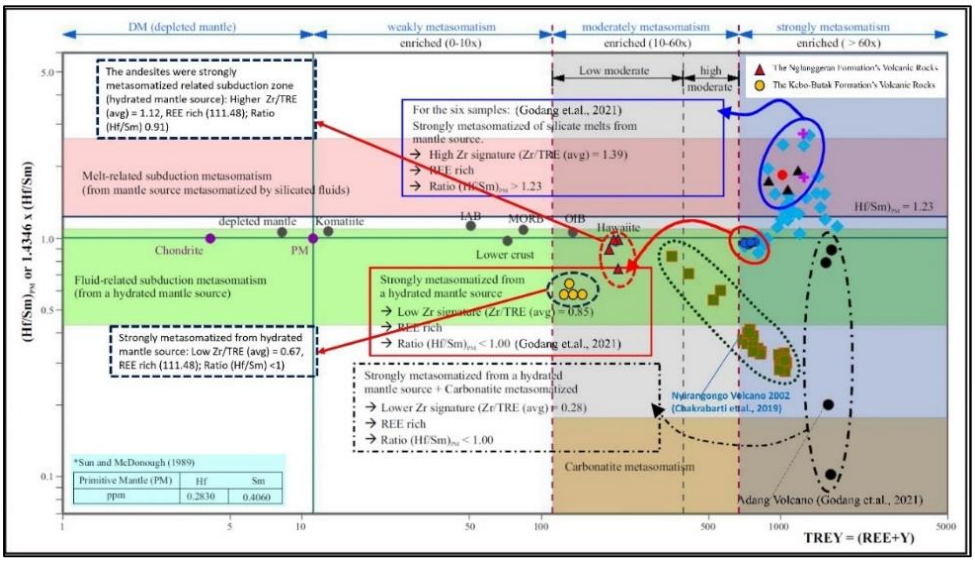

Fig 15. Plot Hf/Sm versus TREY indicates the basaltic volcanic rocks of the Kebo-Butak Formation exposed at the lower Baturagung Range, compared to Adang Volcanic Rocks (Godang et al., 2021), Vulsini Volcanic Rocks (Nappi et al., 1998), madapitic lamphroite (Mitchell et al., 1991), and the Nyirangongo volcanic rocks (Chakrabati et al., 2009), were metasomatized related subduction zone, while the dacitic and andesitic volcanic rocks were formed by strongly metasomatized of a hydrated mantle source.

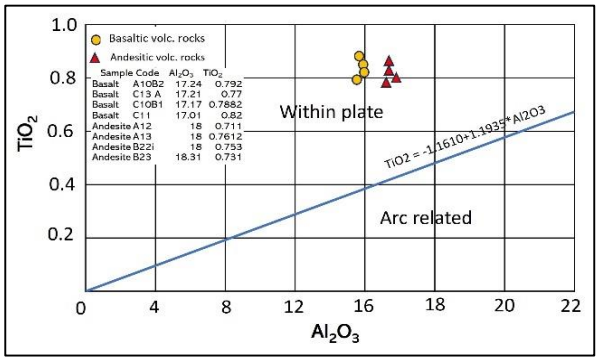

Fig 16. Diagram plot TiO_2 versus Al_2O_3 (Müller and Groves, 1993) for Baturagung Range's volcanic rocks shows within plate relation

Plots Nb/Zr versus Th/Zr (Figure 17) show a depleted mantle source for the basalts and a transition zone for the andesites. Plots Ta/Th versus Th/Hf (Figure 18) according to (Wang, Fan, and Guo, 2003) indicate the basalts were related to continental volcanic arc tectonic setting, and the andesites were by continental extensional zone. A slightly enriched mantle source indicates that it is influenced by a combination of magma mixing resulting from partial melting and the mantle source. An enriched mantle source suggests that the magma was primarily influenced by partial melting occurring within the plate, without significant external contributions from other sources. Plots Ta/Th vs. Th/Hf (Figure 18), according to Wang, Fan, and Guo (2003), these plots suggest that the basalts were related to a continental volcanic arc, while the andesites were associated with a continental extensional zone. This distinguishes a continental volcanic arc from a continental extensional zone, impacted by its composition and origin.

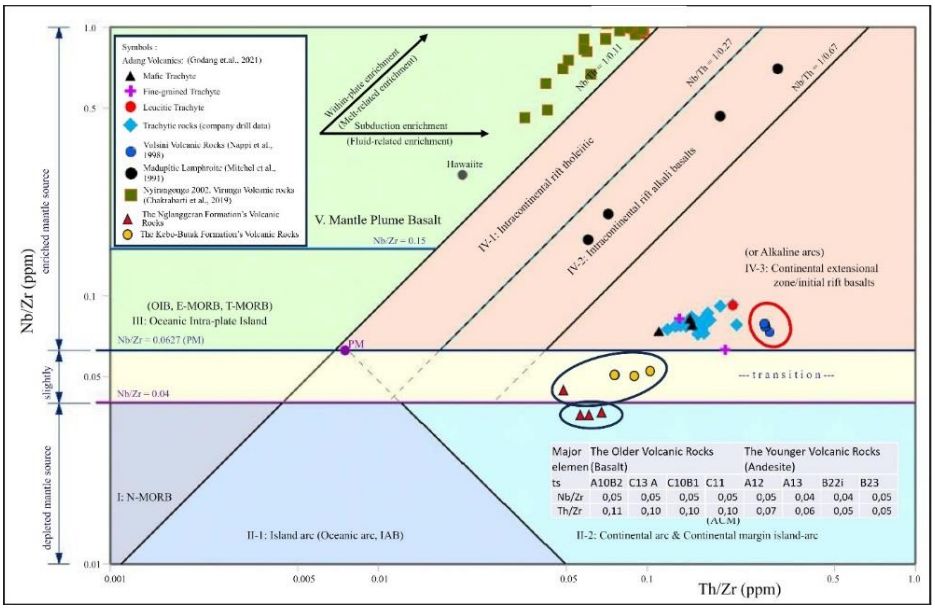

Fig 17. The tectonic discrimination diagram according to (Sun and McDonough, 1989) compared to Adang Volcanic Rocks (Godang et al., 2021), Vulsini Volcanic Rocks (Nappi et al., 1998), madapitic lamproites (Mitchell et al., 1991), and the Nyirangongo volcanic rocks (Chakrabati et al., 2009), suggests the Baturagung Range Volcanic Rocks were related to depleted mantle source and enriched mantle source within a tectonic setting of the transition zone and continental arc & continental margin island arc.

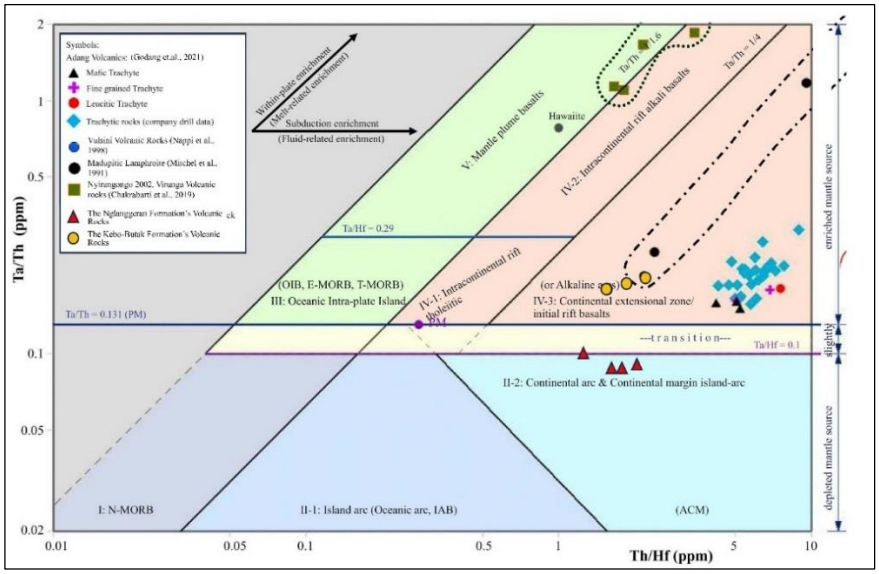

Figure 18. Tectonic discrimination diagram for the Baturagung Range's volcanic rocks according to (Wang et al., 2003a) compared to Adang Volcanic Rocks (Godang et al., 2021), Vulsini Volcanic Rocks (Nappi et al., 1998), madapitic lamproites (Mitchell et al., 1991), and the Nyiragongo volcanic rocks (Chakrabati et al., 2009), suggests a continental volcanic arc to continental extensional zone.

5. Discussion

Circular features in the forms of valley, hogback, and cuesta were described as the center of paleo-volcanoes (Mulyaningsih et al., 2011), (Mulyaningsih and Sanyoto, 2012), (Bronto et al., n.d.), and (Irawan et al., 2009) have explained volcanism in many volcanous in a long period (said during the Neogene) that occurred in the Southern Mountains; as the Kebo-Butak, Semilir, and Nglanggeran Formations. Table 1 explains different relationships; in the west area (Rahardjo et al., 1995b) the 3 formations were continual, in the central area (Surono et al., 1992) displays different geological environments in the same period, and in the east area (Samodra et al., 1992) represents a different time and activities. But all of these old publications informed deep marine Kebo-Butak Volcanism as the earlier, very explosive phase of Semilir Eruptions, and Nglanggeran declining constructive phase. Discussing the Neogene, was a long period of superimposed volcanism; the Neogene Period is the interval between 23-2.6 Ma, which can be divided into two epochs, the Miocene (23-5.3 Ma) and the Pliocene (5.3-2.6 Ma) (Merriam-Webster, 1995). A previous debate is coming from by the events, by a single volcano with single eruption or by so many volcanoes with different eruptions. (Smyth et al., 2005) argued an explosive eruption deposited Semilir Formation during 19-20 Ma, while the Nglanggeran Formation: based on the *Globorotalia binaensis* in the lower Sambipitu Formation, concluded that the volcanic formation has 19-19.8 Ma, so that both Semilir and Nglanggeran Formation were developed in a short time duration (~1 milion year or less).

For the results of this study, stratigraphic and petrologic assessments (thin sections (Fig. 7 and TAS (Fig. 10)) found many magmatic affinities for each volcanic rock formation; basaltic lava (with pillow structures and not) and beds of black tuff, layers of brown crystal tuff (andesitic: with broken shells and glasses), and layers of yellowish-greeny tuff (dacitic) are interpreted that the volcanism deposited the Kebo-Butak Formation was not only by a source but also by many-many sources, although both were originated from a Ca-alkaline magmatic source (Fig. 12). The Harker Diagram shows unrevealed data plots of SiO_2 and K_2O. Those data are unique, by nonlinear of the higher K_2O is not the higher of SiO_2. Those suggest that the Kebo-Butak Formation was not only developed by one period of volcanic activity but also by different volcanoes at different times during the Late Paleogene (Upper Oligocene) to the Early Neogene (Lower Miocene). The long life of the Kebo-Butak Formation (P4-N5) was possibly formed by many volcanoes in different bodies (circulars), which deposited many types and sequences of volcanic materials. So, the Kebo-Butak Formation was formed by several volcanoes with different eruption centers, different periods of activity, and different types of eruptions. The pillow-structured basalt lavas indicate that they were in aquatic environments. Columnar-structured basalt lavas in different areas indicate by effusive eruptions, that where flowed onto the Earth's surface in large volumes, creating lava ponds in many places by many volcanoes. This could be followed by the formation of interbedded basalt lava and black tuff through repeated effusive and phreatic eruptions in a cold aquatic environment. The layers of crystal-rich brown tuff associated with basalt-andesitic lava were formed by phreatic and magmatic eruptions with more viscous andesitic magmas. The beds of white to yellowish-greenish tuff exposed at northern Bantengwareng (near Bayat and Tegalrejo) that associate with zeolite, crystal, and lithic fragments indicate were developed by explosive eruptions. The zeolite indicates a deep alteration to metazomatism.

The volcanic rocks composing the Semilir and the Nglanggeran Formations exhibit physical differences. Petrologically, the volcanic rocks of the Semilir Formation show very fragmented volcanic rocks with color variations: some are dark gray (exposed in Dahromo-Imogiri), gray (in Piyungan-Prambanan Hills), and yellowish-gray to white (in Semilir Hill), mostly in the cuesta nor hogback geomorphologies of the circulars flanks (Fig. 1). The difference colors represent different compositions as described by the thin sections (Fig. 8); a dark color represent dark glass with more content of mafic composition (Fig. 8a, c, d-e), the grey color represent much more quartz and feldspar in the middle area (Fig. 8.b,i), and the white color represent white glass and quartz (Fig. 8.f-h). Those suggest that the Semilir Formation was developed by many volcanoes with many eruptions, but all of them were very explosive. According to (Smyth et al., 2005), in the Semilir Formation ages 19-20 Ma, a violent eruption did not occur in a long period (millions of years), but very short in days, weeks, months, or years of time duration. The historical record can

be found in the Krakatau explosive eruption in August 1883 (Spicak et al., 2008), Tambora in 1815, April 10-11 (2 days) (Raible et al., 2016), and Vesuvius in 79 AD (Sigurdsson et al., 1982) and (Scarpati et al., 2016). The time duration between the previous explosive eruption with the next was not too long, those in less than 500 years. So, it can be concluded that the volcanic rocks composing the Semilir Formation were also produced by more than one eruption in more than one volcano during 20-19 Ma (for a million years).

Stratigraphic and petrologic investigations of the Nglanggeran Formation describe basaltic andesite and andesite; both consist of lava, dike, agglomerate, breccia, and tuff; indicating constructive phase activities, which means dominated by effusive eruptions with less fragmented materials during its activity. The basaltic andesite member and the andesite member are mostly separated by an erosional plane, as an unconformity indication. Some basaltic andesites show a red color that indicates an oxidized area, while others do not. The interpretation is that they were deposited in a subaerial environment or shallow marine settings when sunlight reached the surface. So, the andesites that some show black color as ozidized, but do not occur to others. Some sections show muddy sandstone of the erosional plane, having an age of N 8-9, which can be interpreted as the time gap of volcanisms. The thin sections distinctly reveal their differing properties. A group of basaltic andesites exhibits larger-sized and more abundant aegirine minerals, accompanied by a minor presence of olivines, in porphyritic or poikilitic textures, and vesicular structures. In contrast, andesites have a significantly higher content of glass, a greater amount of andesine, hornblende, and apatites with small grains of aegirine. The basaltic andesites are below the andesite, with a reddish color as a different sequence indication. Furthermore, the basaltic andesites feature a more prominent occurrence of opaque minerals, potentially including titanites, as evidenced by the higher Ti (4800-4940 ppm) than the andesites. As follows, Ca-alkaline volcanic rocks encompass both magnesium-rich and calcium-rich silicate compositions, which are abundant components of the Earth's crust. The major elements show a wide range of SiO_2 compositions, as well as differences in major elements, trace elements, and rare earth elements. Additionally, analysis using the Harker diagrams reveals unique trends for each major element relative to their SiO_2. Plots of Nb/Zr vs. Th/Zr according to (McDonough and Sun, 1995), and Ta/Th vs. Th/Hf according to (Wang et al., 2003b) indicate that were developed within a plate boundary with a slightly enriched mantle source. This confirms that the magmatic activity was influenced by an active continental margin of the Neogene Java Plate, which was mixed with mantle-derived magma. Regarding the volcanic products, this suggests that the volcanisms occurred during the final constructive phase before the subsequent explosive eruptions, resulting in the formation of the circular valleys and domes. The magmatology of the andesitic volcanic rocks differs from that of the basaltic volcanic rocks, although they may have originated from the same magma chamber without further involvement of the mantle source.

A positive trend occurred for plots Al_2O_3, and K_2O indicating further differentiation from lesser K in basaltic andesite to medium K in the andesite phase. A slight positive trend for Na_2O indicates no significant differentiation of the plagioclase. The decrease in Al_2O_3, K_2O, and Na_2O correspond to an increase in SiO_2. This case can be interpreted as the process of magma differentiation, where the initial, more basic magma changes to become more acidic. Negative trends for CaO, MgO, TiO_2, MnO, Fe_2O_3, and P_2O correlate to the higher contents of Ca, Cr, Cu, Ni, V, Ba, and Pb in basaltic andesite than in andesite. Therefore, conversely, the decrease in CaO, MgO, TiO_2, MnO, Fe_2O_3, and P_2O_5 concerning SiO_2 indicates a reduction in these compounds in the magma as SiO_2 increases. Occurrence of assimilation and differentiation, as evidenced by the replacement of augite by aegirine and labradorite by aegirine, transitioning from basaltic andesite to andesite. The volcanic glass-forming minerals in basaltic andesite tend to be darker than in andesite. Negative trends in the TiO_2 plots indicate the occurrence of lithophile minerals as opaque, potentially titanites in augite (Figure 6), as proposed by Grasso *et al.*, (1999), Niu *et al.*, (2018), Liu *et al.*, (2018), and Mullen (1983). This signifies higher concentrations of Ti in basaltic andesite represented by depleted opaque minerals in andesite but abundant in basaltic andesite. The negative trends in the P_2O_5 plots are likely influenced by the presence of appetite. Similarly, negative trends in the MnO plots may be attributed to the presence of manganite (though not significant) or the replacement of Mn^{2+} for Fe_2O_3 in andesite. Notably, the increase in Al_2O_3 for andesite is not accompanied by a linear decrease in TiO_2. The negative trends of MgO and Fe_2O_3 plots exhibit decreasing mafic minerals such as pyroxene and olivine, that depleting in andesite.

As known, the dEu <1 ppm means the enrichment mantle source occurred. The dTa shows 0.1-0.5 represents no interaction with the asthenosphere magma. According to (Godang et al., 2024), dTa >0.8 represents magmatic interaction between the lithosphere with the asthenosphere. The results identify enrichment in LILE (for Cu, Ba, and Sr) but depleted in Ce, Cd, and Sb; enriched in HSFE (high field strength elements) for P, Ti, and Zr, and depleted in Hf and U, also indicate assimilation phase. Indication of enriched aegirine and labradorite for basalt, and higher content of augite and less amounts of plagioclase (in andesite) can be interpreted that the mineral crystalization was controlled under strong metasomatism. The spider diagram that indicates more enrichment in andesite can be interpreted as andesite being younger than basaltic andesite, so there were two sequences of volcanism in the study area during the Nglanggeran Formation.

6. Conclusion

The Baturragung Range was superimposed of volcanisms during the Neogene. Some volcanoes were located above sea level and some others below submarine. The range consists of many volcanoes of different types, different ages, different characteristics, and different magmatism. In contrast, they were developed within the plate boundary with a slightly enriched mantle source in an active continental margin. Their activities were influenced by the mixings of the continental margin with the mantle-derived magmas under strong magmatism of plate boundaries.

Acknowledgments

This research was funded by the Directorate of Research and Community Service, Directorate General of Research and Development Strengthening, Ministry of Education and Culture, Research, and Technology under the Community Service Program Assignment during 2024-2026. Funds were also done in kind by the Ministry of Tourist and Creative Economic Agency, through the village cash labor-intensive program. There are no conflicting interests between the two, so publication can be continued, without causing disputes at a later date. Many thanks are addressed to the DRTPM-Ministry of Education and Culture, Gunungkidul Regency, and the DPPM-Akprind University by the contract research and community services No. 127/E5/PG.02.00/PM.BARU/2024 with the derivative contract No. 0610.21/LL5-INT/AL.04/2024,

01/SPP/DP2M/PKM/VI/2024 and 107/E5/PG.02.00.PL/2024 with the derivative contracts are 0609.24/LL5-INT/AL.04/2024, 03/SPP/DP2M/PL/VI/2024

References

Abuamarah, B.A., Azer, M.K., Asimow, P.D., Shi, Q., 2021. Post-collisional volcanism with adakitic signatures in the Arabian-Nubian Shield: A case study of calc-alkaline Dokhan volcanics in the Eastern Desert of Egypt. Lithos 388, 106051.

Adli, F.Z., Prasetyadi, C., Rachman, M.G., 2018. INCONSISTENT STRATIGRAPHY IN SOUTHERN MOUNTAIN AS AN INDICATION OF OVERTHRUSTING: A CASE STUDY FROM SAMPUNG AREA, PONOROGO, EAST JAVA. Proc. PEKAN Ilm. Tah. IAGI 2018.

Agastya;, I.B.O., Muslih;, Y.B., Muhammad;, R., Pratama, N.M., Hani, I., 2018. BASEMENT STRUCTURES CONTROLLED NEOGENE POST-VOLCANISM CARBONATES IN SOUTHERN MOUNTAIN OF EAST JAVA. Reg. Semin. FOSI.

Akmaluddin, A., Nurhidayah, E.M., Ardian, R., Novian, M.I., Barianto, D.H., 2024. Nannofossil Diversity and Biostratigraphy of Kebo Butak Formation from Kalinampu Area, Bayat-Central Java, in: BIO Web of Conferences. EDP Sciences, p. 4008.

Ardine, J.E., Nugroho, M.O.B., Maulana, M.I., Nugroho, A.N.K., Hisan, N.K., 2022. Deep Marine Reservoir Analog From Semilir Formation Outcrop Data in Ngoro-Oro Area, Gunungkidul, Indonesia.

Ayati, F., Yavuz, F., Asadi, H.H., Richards, J.P., Jourdan, F., 2013. Petrology and geochemistry of calc-alkaline volcanic and subvolcanic rocks, Dalli porphyry copper–gold deposit, Markazi Province, Iran. Int. Geol. Rev. 55, 158–184.

Baba, A.F.., Mulyaningsih, S.., Hidayah, R.A., 2022. Ore Mineralization Characteristics in Hydrothermal Alteration at Mangunharjo and Surrounding Areas, Pacitan, Indonesia. EKSPLORIUM 13–22.

Bachtiar, I.B.O.A.Y., Rizkan, M.M., Pratama, N.M.I.H., n.d. BASEMENT STRUCTURES CONTROLLED NEOGENE POST-VOLCANISM CARBONATES IN SOUTHERN MOUNTAIN OF EAST JAVA.

Barianto, D.H., Kuncoro, P., Watanabe, K., 2010. The use of foraminifera fossils for reconstructing the Yogyakarta graben, Yogyakarta, Indonesia. J. South East Asian Appl. Geol. 2, 138–143.

Bronto, S., 2010. Identifikasi Gunung Api Purba Pendul Di Perbukitan Jiwo, Kecamatan Bayat, Kabupaten Klaten–Jawa Tengah. J. Geol. dan Sumberd. Miner. 20, 3–13.

Bronto, S., Mulyaningsih, S., Hartono, G., Astuti, B., 2009. Waduk Parangjoho dan Songputri: Alternatif Sumber Erupsi Formasi Semilir di daerah Eromoko, Kabupaten Wonogiri, Jawa Tengah. Indones. Jounal Geosci. 4, 77–92.

Bronto, S., Mulyaningsih, S., Hartono, G., Astuti, D.B., n.d. Gunung Api purba Watuadeg: Sumber erupsi dan posisi stratigrafi.

Chakrabati, R., Basu, A., Santo, A.P., Tedesco, D., 2009. Isotopic and geochemical evidence for a heterogeneous mantle plume origin of the Virunga volcanics, Western rift, East African Rift system. Chem. Geol. 259, 273–289.

Chen, L., Zheng, Y.-F., Xu, Z., Zhao, Z.-F., 2021. Generation of andesite through partial melting of basaltic metasomatites in the mantle wedge: Insight from quantitative study of Andean andesites. Geosci. Front. 12, 101124.

Chen, R.D., Suriadi, A.P., Ardenta, H.N., Cahyo, F.A., Rohmana, R.C., 2017. Comparing the Heterogenity Of Volcanogenic Turbidite Deposit in Central Java and East Java for Potential Reservoir Quality Analysis Based on Outcrop Data. Proc. Jt. Conv. MALANG 2017, HAGI – IAGI – IAFMI- IATMI (JCM 2017).

Clements, B., Hall, R., 2007. Cretaceous to Late Miocene stratigraphic and tectonic evolution of West Java.

Clements, B., Hall, R., Smyth, H.R., Cottam, M.A., 2009. Thrusting of a volcanic arc: a new structural model for Java. Pet. Geosci. 15, 159–174.

Cottam, M., Hall, R., Cross, L., Clements, B., Spakman, W., 2010. Neogene subduction beneath Java, Indonesia: Slab tearing and changes in magmatism, in: EGU General Assembly Conference Abstracts. p. 12437.

Dahren, B., Troll, V.R., Andersson, U.B., Chadwick, J.P., Gardner, M.F., Jaxybulatov, K., Koulakov, I., 2012. Magma plumbing beneath Anak Krakatau volcano, Indonesia: evidence for multiple magma storage regions. Contrib. to Mineral. Petrol. 163, 631–651.

Del Marmol, M.-A., 1990. The petrology and geochemistry of Merapi volcano, Central Java, Indonesia.

Dörries, M., 2003. Global science: the eruption of Krakatau. Endeavour 27, 113–116.

Faizal, M., Arisandy, R.F., Tatawu, A.A., Wijaksono, S.H., Alansa, F.R., Arifin, M.N., Mulyaningsih, S., 2018. Efforts on Geological Conservation to Watuadeg-Basalt Pillow Lavas at West Sumber, Berbah District, Sleman Regency, Yogyakarta Special Region-Indonesia. J. Geosci. Eng. Environ. Technol. 3, 174–179.

Godang, S., Priadi, B., Fadlin, F., Van Leeuwen, T., Idrus, A., 2021. Geochemistry Study of Cross-castic Magma Alkalinity Evolution. Indones. J. Geosci. 8, 177–196.

Godang, S., Saputro, S.P., Li, H., 2024. The slab failure in Central Java (Indonesia): New insight into its tectonic setting and origin. Solid Earth Sci. 9, 100199.

Goncalves, D.C., Mulyaningsih, S., 2015. Geologi dan Studi Analisis Porositas Tuff Hitam Formasi Kebobutak Daerah Watugajah dan Sekitarnya Kecamatan Gedangsari Kabupaten Gunung Kidul Daerah Istimewa Yogyakarta., Laporan Penelitian tak-Terpublikasi.

Grasso, V.G., 1968. The TiO2 frequency in volcanic rocks. Geol. Rundschau 57, 930–935.

Harjono, H., Diament, M., Nouaili, L., Dubois, J., 1989. Detection of magma bodies beneath Krakatau volcano (Indonesia) from anomalous shear waves. J. Volcanol. Geotherm. Res. 39, 335–348.

Hartono, G., Bronto, S., 2007. Asal-usul pembentukan Gunung Batur di daerah Wediombo, Gunungkidul, Yogyakarta. Indones. J. Geosci. 2, 143–158.

Husadani, Y.T., Mulyaningsih, S., Bronto, S., 2009. STRATIGRAFI BATUAN GUNUNG API DI DAERAH SINDET DAN SEKITARNYA, DAERAH ISTIMEWA YOGYAKARTA, in: Proceeding Pertemuan Ilmiah Tahunan Ikatan Ahli Geologi Indonesia Ke 39.

Husadani, Y.T., Mulyaningsih, S., Sutikno Bronto, D., n.d. STRATIGRAFI BATUAN GUNUNG API DI DAERAH SINDET DAN SEKITARNYA, DAERAH ISTIMEWA YOGYAKARTA.

Irawan, S.N., Mulyaningsih, S., Bronto, S., Fakhruddin, R., 2009. MENINGKATNYA PENGENDAPAN MATERIAL GUNUNG API PADA MIOSEN TENGAH -MIOSEN AKHIR DI DAERAH SILUK DAN SEKITARNYA, DIY, in: Pertemuan Ilmiah

Tahunan IAGI Ke 39.
Khalaji, A., 2020. Petrology, geochemistry and minearal chemistry of volcanic rocks in the north of Kaboudarahang (Hamedan). Iran. J. Crystallogr. Mineral. 28, 993–1008.
Kusumayudha, S.B., Setyaningrum, T., Rahatmawati, I., Probowati, D., Budiman, L., Nurwantari, N.A., 2023. Assessing the Potential for an Agro-GeoHydroPark in Gedangrejo: An Integrated Geological and Agricultural Study, in: IOP Conference Series: Earth and Environmental Science. IOP Publishing, p. 12029.
La Flèche, M.R., Camire, G., Jenner, G.A., 1998. Geochemistry of post-Acadian, Carboniferous continental intraplate basalts from the Maritimes Basin, Magdalen islands, Quebec, Canada. Chem. Geol. 148, 115–136.
Le Maitre, R.W., Streckeisen, A., Zanettin, B., Le Bas, M.J., Bonin, B., Bateman, P., 2005. Igneous rocks: a classification and glossary of terms: recommendations of the International Union of Geological Sciences Subcommission on the Systematics of Igneous Rocks. Cambridge University Press.
Lucci, F., Rossetti, F., White, J.C., Moghadam, H.S., Shirzadi, A., Nasrabady, M., 2016. Tschermak fractionation in calc-alkaline magmas: the Eocene Sabzevar volcanism (NE Iran). Arab. J. Geosci. 9, 1–12.
McDonough, W.F., Sun, S.., 1995. The composition of the Earth. Chem. Geol. 120, 223–253.
Melaningtyas, G.S.A., Krisnandi, Y.K., Ekananda, R., 2019. Synthesis and characterization of NaY zeolite from Bayat natural zeolite: effect of pH on synthesis, in: IOP Conference Series: Materials Science and Engineering. IOP Publishing, p. 12042.
Merriam-Webster, I., 1995. Merriam-Webster's encyclopedia of literature. Merriam-Webster.
Mitchell, R.H., Bergman, S.C., Mitchell, R.H., Bergman, S.C., 1991. The geochemistry of lamproites. Petrol. Lamproites 295–351.
Mullen, E.D., 1983. MnO/TiO2/P2O5: a minor element discriminant for basaltic rocks of oceanic environments and its implications for petrogenesis. Earth Planet. Sci. Lett. 62, 53–62.
Müller, D., Groves, D.I., 1993. Direct and indirect associations between potassic igneous rocks, shoshonites and gold-copper deposits. Ore Geol. Rev. 8, 383–406.
Mulyaningsih, S., Husadani, Y.T., Devi, L.R., Irawan, S.N., 2009. Analisis distribusi kerusakan akibat gempabumi 27 mei 2006 melalui pendekatan kegunungapian di daerah wonolelo dan sekitarnya, kabupaten bantul, daerah istimewa yogyakarta. Teknol. Technoscientia 1, 248–259.
Mulyaningsih, S., 2019. Identifikasi Jelajah Wisata Geologi Gunung Api Purba Gunung Ireng: Sisi Lain Gunung Api Purba Nglanggeran, Gunungkidul. J. Pariwisata Terap. 3, 136–153.
Mulyaningsih, S., 2016. Volcanostratigraphic Sequences of Kebo-Butak Formation at Bayat Geological Field Complex, Central Java Province and Yogyakarta Special Province, Indonesia. Indones. J. Geosci. Indones. Indone-sian J. Geosci. 3, 77–9477. https://doi.org/10.17014/ijog.3.2.77-94
Mulyaningsih, S., 2015. Vulkanologi.
Mulyaningsih, S., 2013. Interpretasi Gunung Api Komposit Tersier di Pegunungan Selatan mengacu pada Geologi Gunung Api Merapi di Wilayah Daerah Istimewa Yogyakarta. Maj. Geol. Indones. 28, 83–105.
Mulyaningsih, S., Husadani, Y.T., Umboro, P.A., Sanyoto, S., Purnamawati, D.D.I., Teknik, J., 2011. AKTIVITAS VULKANISME EKSPLOSIF PENGHASIL FORMASI SEMILIR BAGIAN BAWAH DI DAERAH JETIS IMOGIRI 4.
Mulyaningsih, S., Muchlis, Heriyadi, N., Kiswiranti, D., 2019. Volcanism in The Pre-Semilir Formation at Giriloyo Region; Allegedly as Source of Kebo-Butak Formation in the Western Southern Mountains. J. Geosci. Eng. Environ. Technol. 4, 217–226.
Mulyaningsih, S., Sanyoto, S., 2012. Geologi Gunung Api Merapi; Sebagai Acuan Dalam Interpretasi Gunung Api Komposit Tersier Di Daerah Gunung Gede-Imogiri Daerah Istimewa Yogyakarta, in: Prosiding Seminar Nasional Aplikasi Sains & Teknologi (SNAST) Periode III ISSN. IST AKPRIND, Yogyakarta, p. B242.
Mulyaningsih, S., Zaim, Y., Juanda Puradimaja, D., Bronto, S., Darwin Alijasa Siregar, D., 2006. Perkembangan Geologi pada Kuarter Awal sampai Masa Sejarah di Dataran Yogyakarta. Indones. Jounal Geosci.
Nandaka, I.G.M.A., Gertisser, R., Walter, T.R., Troll, V.R., Ratdomopurbo, A., 2023. Merapi: Evolving knowledge and future challenges, in: Merapi Volcano: Geology, Eruptive Activity, and Monitoring of a High-Risk Volcano. Springer, pp. 553–572.
Nappi, G., Antonelli, F., Coltorti, M., Milani, L., Renzulli, A., Siena, F., 1998. Volcanological and petrological evolution of the eastern Vulsini district, central Italy. J. Volcanol. Geotherm. Res. 87, 211–232.
Niu, H., Sato, H., Zhang, H., Ito, J., Yu, X., Nagao, T., Terada, K., Zhang, Q., 2006. Juxtaposition of adakite, boninite, high-TiO2 and low-TiO2 basalts in the Devonian southern Altay, Xinjiang, NW China. J. Asian Earth Sci. 28, 439–456.
Novianto, A., Yogafanny, E., Ernawati, R., Nandari, W.W., 2020. Brackishwater in the Jambakan area: Where did they come from?(geoelectric and geohydrology analysis), in: AIP Conference Proceedings. AIP Publishing.
Novita, D., Barianto, D.H., Novian, M.I., 2014. Planktonic Foraminifera Biozonation of the Middle Eocene-Oligocene Kebo Formation, Kalinampu Area, Bayat, Klaten, Central Java. Ber. Sedimentol. 31, 70–81.
Nugraha, A.M.S., Hall, R., 2012. Cenozoic History of the East Java Forearc. PROCEEDINGS, Indones. Pet. Assoc. IPA12-G-028.
Nugrahini, A., Inaniawardani, V., Sulaksana, N., Sudrajad, A., 2017. The First Period of Volcano Activity in Semilir Formation of Southern Mountain of Java Basin, in: Proceedings of the 2nd Join Conference of Utsunomiya University AndUniversitas Padjadjaran. pp. 256–261.
Nugrahini, A., Isnaniawardhani, V., Sudradjat, A., Sulaksana, N., 2019. CHARACTERISTICS OF SEMILIR FORMATION IN RELATIONSHIP WITH THE PERIOD OF VOLCANIC ACTIVITY. GEOMATE J. 16, 154–162.
Paryani, E., Haryono, E., 2022. Analysis of Cave Morphology in Wediombo and its Surrounding Area, Gunungkidul, in: IOP Conference Series: Earth and Environmental Science. IOP Publishing, p. 12053.
Patria, A.A., Maulana, A., Islamiyati, D., Dwi, B., Cahya, M., Novian, I., n.d. Volcanostratigraphy of Semilir Formation: A Key to Predict Ancient Volcanic Eruption. FOSI-IAS-SEPM Reg. Semin.
Pearce, J.A., 1996. A user's guide to basalt discrimination diagrams. Trace Elem. geochemistry Volcan. rocks

Appl. massive sulphide Explor. Geol. Assoc. Canada, Short Course Notes 12, 113.
Peccerillo, A., Taylor, S.R., 1976. Geochemistry of Eocene calc-alkaline volcanic rocks from the Kastamonu area, northern Turkey. Contrib. to Mineral. Petrol. 58, 63–81.
Rahardjo, W., Sukandarrumidi, R.H.M.D., Rosidi, H.M.D., 1995a. Geological map of the Yogyakarta sheet.
Rahardjo, W., Sukandarrumidi, Rosidi, H., 1995b. Yogyakarta Sheet Geological Map scale 1: 100.000. Bandung Geol. Res. Dev. Cent.
RAHMAD, B., HANANTO, H., NUGROHO, T., PRAMONO, S.H., SUMANTRI, A., 2017. Shale Hydrocarbon Potential of Semilir Formation in Buyutan, Klaten, Central Java, Indonesia. Int. Symp. Earth Sci. Technol. 2017.
Raible, C.C., Brönnimann, S., Auchmann, R., Brohan, P., Frölicher, T.L., Graf, H., Jones, P., Luterbacher, J., Muthers, S., Neukom, R., 2016. Tambora 1815 as a test case for high impact volcanic eruptions: Earth system effects. Wiley Interdiscip. Rev. Clim. Chang. 7, 569–589.
Razi, M.H.M., 2018. Geology and depositional environment of Nglanggeran Formation in Gunung Kidul Regency, Yogyakarta, Indonesia.
RODHI, A., Indrajaya, E., PRASETYADI, C., SETIAWAN, J., Pratiknyo, P., 2016. Fractures Control of Groundwater Aquifer Configuration at Baturagung Volcanic Range, A Potential New Geosite of Gunung Sewu Geopark.
Rohayati, R., Krisnandi, Y.K., Sihombing, R., 2017. Synthesis of ZSM− 5 zeolite using Bayat natural zeolite as silica and alumina source, in: AIP Conference Proceedings. AIP Publishing.
Romario, I.F.B., Mindasari, D., Suprapto, R.E., Yusuf22, M.A., 2015. Oligo-Miocene Tectonic of Java and The Implication for Flexural Basin of Southern Mountain in Affecting Depositional System in Kerek Formation, in: Proceedings Joint Convention Balikpapan.
Salim, F.N., 2020. Geology and deposition of volcaniclastic in Nglanggeran formation at Patuk Area, Gunung Kidul, Yogyakarta, Indonesia.
Samodra, H., Gafoer, S., Tjokrosapoetro, S., 1992. Peta Geologi Lembar Pacitan, Jawa, skala 1: 100.000. Puslitbang Geol. Bandung.
Scarpati, C., Perrotta, A., De Simone, G.F., 2016. Impact of explosive volcanic eruptions around Vesuvius: a story of resilience in Roman time. Bull. Volcanol. 78, 1–6.
Self, S., Rampino, M.R., Newton, M.S., Wolff, J.A., 1984. Volcanological study of the great Tambora eruption of 1815. Geology 12, 659–663.
Setijadji, L.D., Kajino, S., Imai, A., Watanabe, K., 2006. Cenozoic island arc magmatism in Java Island (Sunda Arc, Indonesia): Clues on relationships between geodynamics of volcanic centers and ore mineralization. Resour. Geol. 56, 267–292. https://doi.org/10.1111/j.1751-3928.2006.tb00284.x
Sheth, H.C., Torres-Alvarado, I.S., Verma, S.P., 2002. What Is the "Calc-alkaline Rock Series"? Int. Geol. Rev. 44, 686–701. https://doi.org/10.2747/0020-6814.44.8.686
Sigurdsson, H., Cashdollar, S., Sparks, S.R.J., 1982. The eruption of Vesuvius in AD 79: reconstruction from historical and volcanological evidence. Am. J. Archaeol. 86, 39–51.
Smyth, H., Hall, R., Hamilton, J., Kinny, P., 2005. East Java: Cenozoic basins, volcanoes and ancient basement.
Smyth, H.R., Hall, R., Nichols, G.J., 2008. Cenozoic volcanic arc history of East Java, Indonesia: The stratigraphic record of eruptions on an active continental margin. Spec. Pap. Soc. Am. 436, 199.
Smyth, H.R., Hamilton, P.J., Hall, R., Kinny, P.D., 2007. The deep crust beneath island arcs: inherited zircons reveal a Gondwana continental fragment beneath East Java, Indonesia. Earth Planet. Sci. Lett. 258, 269–282.
Soeria-Atmadja, R., Maury, R.C., Bellon, H., Pringgoprawiro, H., Polve, M., Priadi, B., 1994. Tertiary magmatic belts in Java. J. Southeast Asian Earth Sci. 9, 13–27.
Soviana, N.N., Brahmantyo, B., Abdurrachman, M., Sabila, D., Firman, S.N., 2020a. "Gunung Api Purba Nglanggeran" welcomes UNESCO Global Geopark Reassessment in 2019, in: IOP Conference Series: Earth and Environmental Science. IOP Publishing, p. 12025.
Soviana, N.N., Brahmantyo, B., Abdurrachman, M., Sabila, F.S.N., 2020b. "Gunung Api Purba Nglanggeran" welcomes UNESCO Global Geopark Reassessment in 2019, in: IOP Conference Series: Earth and Environmental Science. IOP Publishing, p. 12025.
Spicak, A., Kozák, J., Vank, J., Hanus, V., 2008. The Krakatau volcano 125 years after the catastrophic eruption (August 27, 1883). Stud. Geophys. Geod. 52, 449.
Sun, S.-S., McDonough, W.F., 1989. Chemical and isotopic systematics of oceanic basalts: implications for mantle composition and processes. Geol. Soc. London, Spec. Publ. 42, 313–345.
Surono, S., 2009. Litostratigrafi Pegunungan Selatan Bagian Timur Daerah Istimewa Yogyakarta dan Jawa Tengah. J. Geol. Dan Sumberd. Miner. 19, 209–221.
Surono, S., 2008. Sedimentasi Formasi Semilir di Desa Sendang, Wuryantoro, Wonogiri, Jawa Tengah. J. Geol. dan Sumberd. Miner. 18, 29–41.
Surono, Toha, B., Sudarno, I., 1992. Peta Geologi Lembar Surakarta-Giritontro, Jawa. Bandung Pus. Penelit. dan Pengemb. Geol.
Sutarto, S., Soesilo, J., 2020. Atlas Batuan Pegunungan Jiwo, Bayat, Kabupaten Klaten, Jawa Tengah.
Syafitri, A., Sucipta, I., Arifa, A.N., Saepuloh, A., Widiyantoro, S., 2022. Tectonic Setting of Mount Agung, Bali: Insight From Petrology and Geochemistry Analysis, in: IOP Conference Series: Earth and Environmental Science. IOP Publishing, p. 12005.
van Bemmelen, R.W., 1949. General Geology of Indonesia and adjacent archipelagoes. Geol. Indones.
Wang, Y., Fan, W., Guo, F., 2003a. Geochemistry of early Mesozoic potassium-rich diorites-granodiorites in southeastern Hunan Province, South China: Petrogenesis and tectonic implications. Geochem. J. 37, 427–448.
Wang, Y., Fan, W., Guo, F., Peng, T., Li, C., 2003b. Geochemistry of Mesozoic mafic rocks adjacent to the Chenzhou-Linwu fault, South China: implications for the lithospheric boundary between the Yangtze and Cathaysia blocks. Int. Geol. Rev. 45, 263–286.
Wulaningsih, T., Humaida, H., Harijoko, A., Watanabe, K., 2013. Major element and rare earth elements investigation of Merapi Volcano, Central Java, Indonesia. Procedia Earth Planet. Sci. 6, 202–211.